3D hydrogeological reconstruction of the fault-controlled Euganean Geothermal System (NE Italy)

Torresan Filippo [a], Piccinini Leonardo [a,b*], Pola Marco [c], Zampieri Dario [a,b], Fabbri Paolo [a,b]

a. Department of Geosciences, Università degli Studi di Padova, Via Giovanni Gradenigo, 6, 35131, Padova, Italy
b. Geothermal System Hydrostructures (GSH), Interdepartmental Centre "Giorgio Levi Case" for Economics and Technology, Università degli Studi di Padova, Italy
c. Croatian Geological Survey, Sachsova 2, 10000 Zagreb

Corresponding author: leonardo.piccinini@unipd.it

Abstract

The assessment of renewability in geothermal and hydrogeological resources is a particular requirement for their future preservation. The sustainable exploitation of a geothermal resource for its long-term utilization is related to both the water demand and the hydrogeological characteristics of the geothermal field, while its renewability is more influenced by the geological and hydrogeological processes that enhance the groundwater flow. Numerical modeling can be successfully used to assess both the impact of the processes occurring in the geothermal system and the renewability of the associated resources. However, the reliability of a numerical simulation is influenced by the accuracy of the dataset used to reproduce the geological system. A 3D hydrogeological reconstruction model, rather than a simplified conceptualization of the geological setting, can increase the consistency of the modeling results. In the case of the Euganean Geothermal System (NE Italy), a detailed reconstruction was performed to quantitatively reproduce the hydrogeological elements that allow the development of the geothermal system and to estimate the amount of thermal waters stored in the reservoir. The structural setting of the central Veneto region, in particular the high-angle NNW-trending faults of the Schio-Vicenza Faults System, play a fundamental role in the existence of the Euganean Geothermal System permitting the hydraulic connection between the recharge area and the exploitation field. In addition, regional and local scale faults and fractures favour the fluid convection that represent the main process warming the thermal fluids. Reproducing such complex geological setting in a 3D model allows to improve the knowledge on the features that characterize the geothermal system and to attain a solid framework for the construction of a 3D regional numerical model that will be used to assess the renewability of the system. *Keywords: 3D Hydrogeological Reconstruction, Renewability, MOVE Software, Euganean Geothermal System*

1. Introduction

Energy production from renewable resources is a unique aspect of the 21st century that favors the replacement of conventional fossil resources, the reduction of greenhouse gas emissions, and the protection of the environment (Huenges, 2010; International Energy Agency, 2019). Geothermal resources are the most important renewable geological resource, and they are used worldwide for energy production, industrial processes, district heating, and balneology (Lund and Boyd, 2016). Sustainable exploitation is crucial to guarantee their long-term utilization, future maintenance, and environmental protection (Axelsson, 2010; Limberger et al., 2018; Rybach, 2003; Rybach and Mongillo, 2006). The term renewable describes the property of the resource and is related to the regional geological and hydrogeological processes that allow for its development. In contrast, the term sustainable refers to how the resource is utilized (Monterrosa and Montalvo López, 2010; Stefansson, 2000). The sustainable use of a natural resource can be achieved through the implementation of a site-specific management plan that accounts for the local hydrogeological characteristics of the system, the energy demand, and the long-term exploitation (Monterrosa and Montalvo López, 2010; Rybach, 2003). To achieve a sustainable utilization, the amount of exploited water (and energy) must be lower or equal to the renewable recharge of the system (Monterrosa and Montalvo López, 2010). Consequently, the processes allowing for the existence and renewability of a geothermal system should be carefully evaluated before starting the resource exploitation (Cataldi, 2001; Monterrosa and Montalvo López, 2010).

The impact of the exploitation on the geological and physical processes is usually evaluated through numerical simulations that should include all features characterizing the system (Axelsson, 2010; Franco and Vaccaro, 2014; Monterrosa and Montalvo López, 2010; O'Sullivan et al., 2010). The capability of the numerical model to reproduce these processes and to evaluate the possible utilization scenarios is strictly related to the reliability and accuracy of the input dataset (Axelsson, 2010). The dataset generally includes geological and geophysical data for the subsurface reconstruction and hydrogeological and thermal data for the parameterization of the physical properties. The interpretation of geological and geophysical data and their integration in a 2D framework consisting of maps and sections is a simple and cost-effective strategy to obtain a reliable reconstruction of the regional geological settings driving geothermal fluid circulation. It is more complex to define the conceptual hydrogeological or geothermal model and, above all, translate it into a numerical model. In fact, the crucial aspect of the numerical implementation is the degree of simplifications imposed by the rules of numerical discretization or by the need of reducing the computational effort. The typical issue in numerical modeling is the representation of discontinuities (i.e., faults, thrusts, fractured zones) through a continuous structure, such as the traditional finite difference grid or the finite element mesh. Recently, the use of unstructured meshes made of tetrahedral elements improved the capability of reproducing the complex geometries and heterogeneities that typically occur in a geothermal system (Blöcher et al., 2010; Cacace and Blöcher, 2015; Ingebritsen et al., 2010; Painter et al., 2012; Painter et al., 2016; Passadore et al., 2012; Volpi et al., 2018). This new discretization approach can become particularly profitable when used together with a detailed 3D reconstruction of the geothermal reservoir made with specific tools, such as MOVE (Midland Valley Exploration Ltd.), PETREL (Schlumberger), or SKUA-GOCAD

(Paradigm). Nowadays, detailed 3D geological and hydrogeological reconstructions are profitably used for estimating the reservoir and water volumes and for groundwater flow and contaminant transport modeling (Cushing et al., 2020; Ghiglieri et al., 2016; Hassen et al., 2016; Høyer et al., 2019; Martínez-Martínez et al., 2017; Moya et al., 2014; Thierry et al., 2009; Touch et al., 2014; Zhang and Zhu 2018).

The Euganean Geothermal System (EuGS) is a regional geothermal system extending for a length of about 100 km in the central part of the Veneto region (NE Italy). The associated geothermal resource is one of the most important low enthalpy, water-dominated, geothermal resources in Italy, and it is exploited in the Euganean Geothermal Field (EuGF). The EuGF is located southwest of Padua, covering an area of approximately 25 km^2 to the east of the Euganean Hills (Fig. 1). Euganean thermal waters have been used for therapeutic purposes since the Roman era, and currently, approximately 15 M-m^3 per year of these thermal waters with temperatures from 63 °C to 87 °C are being exploited by approximately 150 wells (Fabbri et al., 2017). The thermal waters are utilized for recreational purposes and secondarily for aquaculture, floriculture and heating of buildings. The income of the related tourism activities is 300 million euros per year (Consorzio Terme Euganee, 2016), confirming the importance of this natural resource on the regional economy.

The forced extraction of the thermal waters started at the end of the 19th century. The increasing water demand caused a decrease in the potentiometric level in the 1960s and 1970s, depleting the thermal reservoirs. Subsequently, the decrease in exploitation in the 1990s allowed the recovery of the potentiometric level up to a few meters below the ground level. This recovery was due to a reduction in the water demand by the tourism industry and to the regulation of the extracted volumes imposed by the Veneto Region administration (Fabbri, 2001; Fabbri et al. 2017; Fabbri and Trevisani 2005; Pola et al. 2015a). The utilization of reinjection wells for re-establishing the natural condition of the system (Diaz et al. 2016; Kaya et al. 2011; Limberger et al. 2018) was excluded due to (i) the peculiar hydrogeological settings of the EuGF and (ii) the high density of pumping wells. In fact, reinjection into a highly exploited system might lead to thermal feedback phenomena, diminishing the quality of the resource. The sustainability of exploitation in the EuGF is essentially controlled by the amount of extracted water, the local geological and hydrogeological conditions, and the renewability of the system. Consequently, the definition of a sustainable management plan is essential for the preservation of this resource.

The important role played by the hydrogeological conditions on the development of the EuGS, due to the concomitant interaction of several geological structures, increases the need for a hydrogeologically reliable implementation of the conceptual model in a numerical framework. This work details the hydrogeological reconstruction of the EuGS, which is preliminary to the numerical implementation through an unstructured mesh. The term hydrogeological reconstruction takes into consideration the hydrostratigraphic setting characterizing the EuGS and the main regional tectonic structures that constitute the central part of the Veneto region. Different types of geological and geophysical data (geological and seismic sections, stratigraphic logs, and geological, structural and gravimetric maps) were used to perform this reconstruction. Considering the large size of the study area (approximately 5,700 km^2), the employed approach provides (i) the subdivision of the geological sequence characterizing the Veneto region in several hydrostratigraphic units, considering the hydraulic properties of each unit, and (ii) the representation of only the main regional scale tectonic structures. The hydrogeological reconstruction was performed to: (i) evaluate the role played by the main regional faults on the development of the EuGS; (ii) validate the currently existing EuGS hydrogeological conceptual model, and (iii) estimate the groundwater volume in the thermal reservoir, considering the total volume of the aquifer and making some hypotheses on its effective porosity.

2. Geological and hydrogeological setting

The stratigraphic sequence of the Veneto region is characterized by Permian to Pliocene sedimentary formations that are composed mostly of limestones, dolostones, and marlstones (Antonelli et al., 1990). In addition, two main volcanic cycles affected this area: (i) the Middle Triassic effusive volcanic phase, dominated by felsic products (De Vecchi and Sedea, 1983), and (ii) the Paleogene magmatic cycle with mafic to ultramafic effusive rocks in the Lessini area (De Vecchi and Sedea, 1995) and alkaline to subalkaline bodies in the Euganean area (Bartoli et al., 2015; Bellieni et al., 2010). The stratigraphic sequence lies on a basement composed of pre-Permian phyllites and micaschists rocks and it is closed to the top by Pleistocene to Present alluvial deposits of the Veneto plain (Antonelli et al., 1990).

Two main structural domains characterize this area: the Eastern Southern Alps, which are affected by south-verging structures (Castellarin and Cantelli, 2000), and their foreland (Fig. 1). The transition between these domains is marked by a set of ENE-WSW trending, NNW dipping thrusts (Fig. 1). The Veneto foreland (Fig. 1) is composed of two distinct elements: the slightly deformed Lessini-Berici-Euganei structural high (LBE) and the deformed foredeep (Veneto plain foredeep). These elements are separated by the Schio-Vicenza Faults System (SVFS; Pola et al., 2014a), a system of NNW-SSE trending, NNE dipping, and high-angle faults (Fig. 1). The most prominent segment is the Schio-Vicenza fault (SV), which marks the sharp and rectilinear transition between the LBE reliefs and the Veneto plain, while other segments are buried beneath the alluvial plain (Conselve-Pomposa, CP, and Travettore-Codevigo, TC). This system of faults developed during the extensional phases related to the Norian – Early Cretaceous thinning of the Adria passive margin and to the Paleogene magmatism (Zampieri and Massironi, 2007). The interaction between two main segments of the SVFS (SV and CP in Fig. 1) developed a left stepover structure (relay ramp) to the south of Padua (Zampieri et al., 2009). This structure accommodated the regional extension, favoring the strain transfer from one fault segment to the other (Fossen and Rotevatn, 2016). Subsequently, during the Neogene shortening associated with the indentation of the Northern Adria margin against the European plate (Mantovani et al., 2009), the NNW-SSE trending faults were reactivated with sinistral strike-slip kinematics (Massironi et al., 2006; Zampieri et al., 2003; Zampieri and Massironi, 2007). The inherited relay ramp was reactivated and deformed by a network of interconnected small-scale fractures and larger-scale faults, resulting in a breached relay ramp (Pola et al., 2020). This local pattern is constituted by NNE-SSW, ESE-WNW, and NW-SE trending faults (Pola et al., 2014b) representing a “Hill-type” mixed extensional/shear-extensional fracture mesh (Hill, 1977).

In detail, considering the outcropping formations in the Euganean Hill (Cucato et al., 2012) and the data derived from the stratigraphic logs of thermal wells, the stratigraphic sequence of the EuGF is composed of (i) Quaternary alluvial cover, with a maximum thickness of approximately 200 m; (ii) Torreglia Formation (Lower Eocene – Lower Oligocene); (iii) Scaglia Rossa Formation (Upper Cretaceous – Middle Eocene); (iv) Scaglia Variegata Alpina Formation (Lower – Upper Cretaceous); (v) Maiolica Formation (Upper Jurassic – Lower Cretaceous); (vi) Rosso Ammonitico Formation (Upper Jurassic); (vii) Calcari Grigi Group (Lower – Middle Jurassic), and (viii) Dolomia Principale Formation (Upper Triassic). Generally, formations (ii), (iii), and (iv) are constituted by marly limestones and mudstones, whereas formations (v), (vi), (vii), and (viii) are mainly composed of limestones and dolostones. Moreover, the stratigraphic sequence is intruded by volcanic rocks (i.e., trachyte, rhyolite, basalt, and latite) of the Paleogene volcanic cycle. From a hydrogeological perspective, marly limestones and mudstone may be considered aquitards, while limestones and dolostones are aquifers. In particular, thermal waters are exploited from two fractured reservoirs located at different depths. The first aquifer, which represents the most exploited thermal aquifer, is located in the Maiolica Formation at depths from 300 m to 600 m, and its transmissivity varies between 13 m^2/day and 500 m^2/day (Fabbri, 1997). The second aquifer is situated in the Calcari Grigi and Dolomia Principale formations at a depth between 800 m and 1,000 m (Pola et al., 2015b), but it is less explored and exploited.

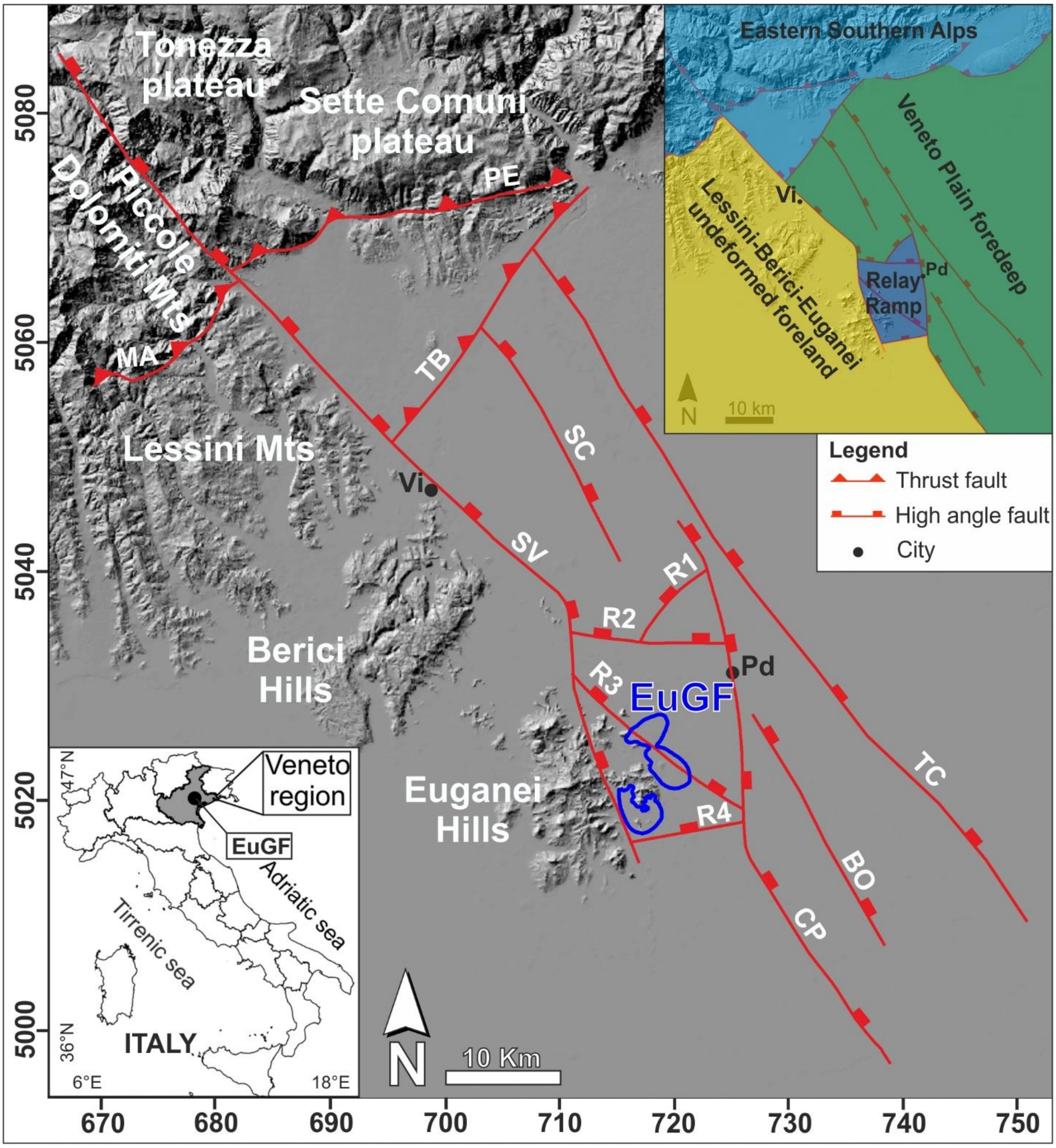

Fig. 1 Structural sketch of the central Veneto region (NE Italy in the lower left insert) showing the principal faults of the study area (SV = Schio-Vicenza fault; SC = Sandrigo-Camisano fault; TC = Travettore-Codevigo fault; BO = Bovolenta fault; CP = Conselve-Pomposa fault; R1 = Relay ramp fault 1; R2 = Relay ramp fault 2; R3 = Relay ramp fault 3; R4 = Relay ramp fault 4; MA = Marana thrust; PE = Pedemontana thrust; TB = Thiene-Bassano thrust) and the resulting structural domains (upper right insert). The main cities (Pd = Padua; Vi = Vicenza) and the Euganean Geothermal Field (EuGF) are also shown. The coordinates of the map are in the UTM zone 32N system using the WGS84 datum.

2.1 Hydrogeological conceptual model

The hydrogeological conceptual model proposed by Pola et al. (2015b) suggests that the EuGF represents the terminal portion of the regional-scale EuGS. Thermal waters are of meteoric origin, infiltrating at an altitude of approximately 1,500 m a.s.l., as suggested by their stable isotope composition (Gherardi et al., 2000). For this reason, the recharge area was located in the Veneto Prealps (i.e., Tonezza and Sette Comuni Plateaus) to the E of the SV fault (Fig. 1).

The proposed recharge area is characterized by dense fracturing and a well-developed karst system (Aurighi et al., 2004; Barbieri and Grandesso, 2007). These features increase the permeability of the outcropping Mesozoic limestones and dolostones, favoring the deep infiltration of meteoric waters.

The thermal waters flow toward the exploitation field mainly into the Mesozoic formations, but a secondary flow within the underlying evaporitic formations probably occurs, as suggested by the correspondence between the Ca/SO_4 ratio of waters and the gypsum-anhydrite reference value (0.46 ± 0.4 and 0.42, respectively; Gherardi et al., 2000). The southward migration of the thermal fluids is enhanced by the damage zone of the SV fault, which is characterized by a network of secondary fractures producing a local high permeability field.

In the EuGF area, the hydrothermal waters intercept the pattern of fractures deforming the relay ramp. These fractures represent a favorable way to increase the thermal fluids inflow inside the exploited reservoirs. The warming of the thermal fluids is mainly attributed to (i) locally enhanced convection occurring in the relay ramp subsurface favored by fracturing (Pola et al., 2020), and (ii) slightly anomalous regional crustal heat flow (70-80 mW/m^2; Pasquale et al., 2014).

3. Materials and methods

The first step in the 3D hydrogeological reconstruction of the EuGS is the choice of the model domain. The domain should include the main elements of the system (i.e., recharge area in the Prealps and outflow area in the EuGF) and the geological features favoring the circulation of the thermal fluids. The model domain was extended by a few tens of kilometers S of the EuGF and W and E of the SV and CP footwall and hanging wall to achieve a more complete regional reconstruction. This area is approximately 115 km long and 50 km wide (Fig. 2), and the depth was set to 9 km. The extension in depth was constrained by the analysis of seismic sections (Pola et al., 2014a), locating the transition between the sedimentary formations and the pre-Permian crystalline basement at a maximum depth of 8 km.

Within the model domain, the data (Table 1) used to perform the hydrogeological reconstruction consist of (i) gravimetric maps, (ii) geological and structural maps, (iii) well logs up to 5 km deep (Fig. 2; Table 2), and (iv) geological and seismic sections (Fig. 2). Gravimetric and structural maps and seismic sections were used to define the structural setting of the analyzed geothermal system. Considering the role of the regional fault systems on the development of the EuGS, the structural reconstruction represented a fundamental step in the performed modeling.

Deep wells are scattered in the Veneto plain (8 wells in approximately 3,500 km^2) and are absent in the Prealps (Fig. 2). Consequently, the stratigraphic logs of these wells are not favorable for the detailed reconstruction of the regional geological setting. However, these data were combined with the stratigraphic columns of geological maps to group the formations of the Veneto region sequence into different hydrostratigraphic units based on their hydrogeological behavior and their role in the development of the EuGS. Well data were also used to validate the performed reconstruction.

Cross-sections from geological maps and seismic sections were used to perform the hydrogeological reconstruction. These cross-sections were reinterpreted using the aforementioned hydrostratigraphic unit discretization and considering the degree of detail required for a regional model. In addition, new hydrogeological sections were built from geological and structural maps to detail the reconstruction in areas without available sections.

The hydrogeological reconstruction was performed using MOVE software (Midland Valley Exploration Ltd.). This software develops three-dimensional geological reconstructions starting from different types of data (i.e., geological and seismic sections, well data, etc.). The base of each hydrostratigraphic unit and the main fault planes were built using a tool that constructs a surface between a group of lines, for example the base of a unit in adjacent sections, using the Delaunay triangulation.

The regional faults were used as internal boundaries of the domain for the reproduction of the hydrostratigraphic setting. As seen in Fig. 1, the central part of the Veneto region can be subdivided into 4 main structural domains (i.e., Eastern Southern Alps, Lessini-Berici-Euganei block, Veneto plain foredeep, and relay ramp). Since the displacement along the bordering faults is generally high, these areas were modeled separately. The reconstructions of two adjacent domains were merged using the common faults as constraints. During this step, particular attention was paid to maintaining the correct fault kinematics between juxtaposed domains.

After the reconstruction validation, the 3D hydrogeological reconstruction was employed to quantify the groundwater availability in the reservoir. The volume of the hydrostratigraphic units representing the thermal reservoir was estimated, and three scenarios were considered: (i) the volume in the whole modeled area; (ii) the volume within the interaction zone, and (iii) the volume delimited by the EuGF. The volumes were reconstructed in the MOVE software using a regular-shaped tetrahedral mesh. Subsequently, some hypotheses on effective porosity (n_e) were made. The n_e values were estimated from the work of Pasquale et al. (2011) and from the geological information obtained by the analysis of the Villaverla 1 and Legnaro 1 wells (Fig. 2). The minimum, mean, and maximum values of n_e were considered. The groundwater available in the three scenarios was estimated by multiplying the aquifer volume by the n_e values.

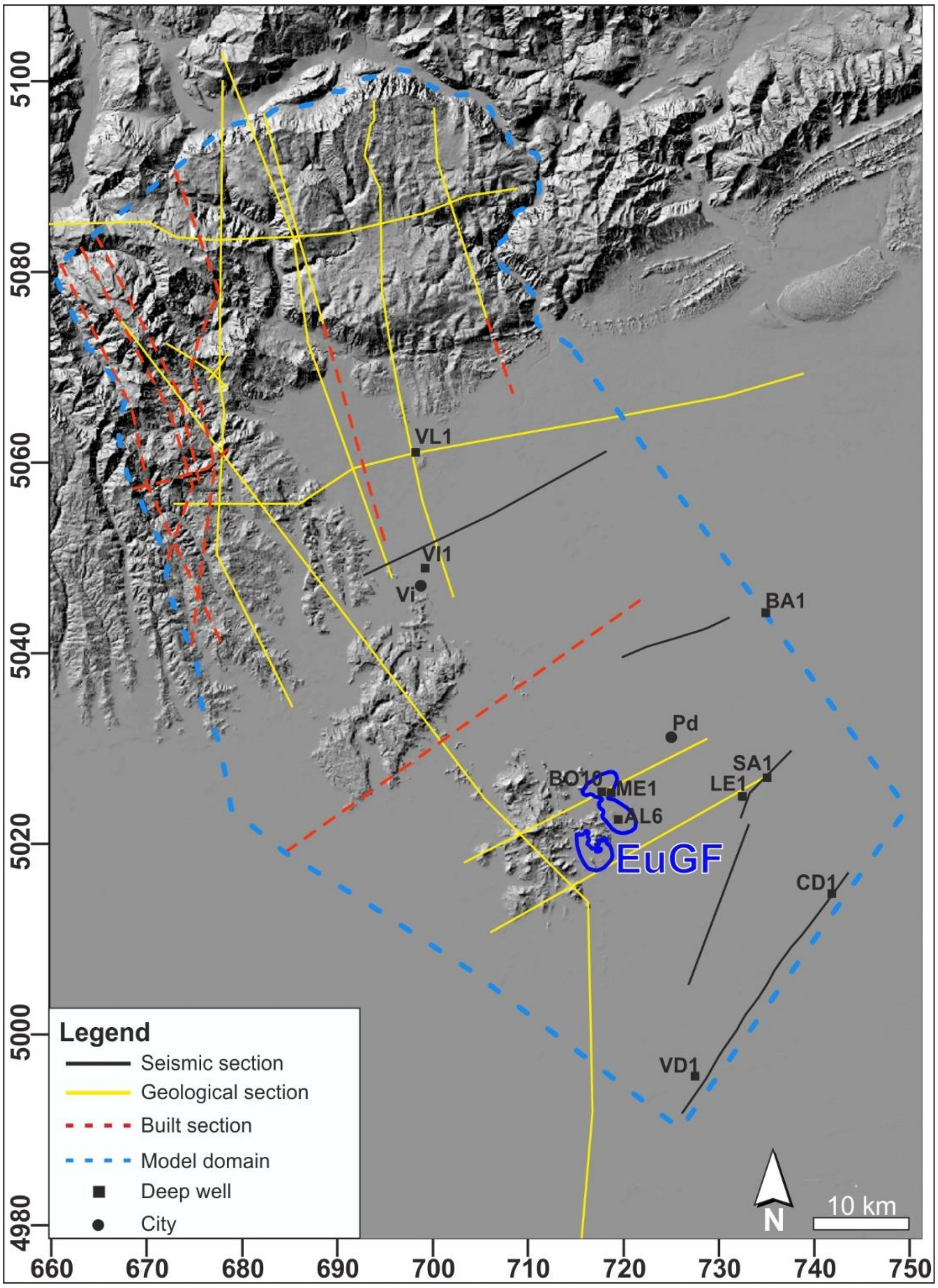

Fig. 2 Area of the model domain and data utilized for the 3D hydrogeological reconstruction. The well acronyms are reported in Table 2. The main cities of the study area (Pd = Padua, Vi = Vicenza) and the Euganean Geothermal Field (EuGF) are shown. The coordinates are in the UTM zone 32N system using the WGS84 datum.

Table 1 Data used to perform the 3D hydrogeological reconstruction.

TYPE OF DATA	SOURCE
Digital Elevation Model	Veneto Region WebGIS (https://idt2.regione.veneto.it/)
Geological Map and Geological Section	Geological Map of Veneto Region (1:250,000; Antonelli et al., 1990); Geological Map of Asiago (1:50,000; Barbieri and Grandesso, 2007); Geological Map of Recoaro (1:20,000; Barbieri et al., 1980); Geological Map of Valli-Posina-Laghi (1:20,000; Sedea and Di Lallo, 1984); Geological Map of Euganean Hill (1:25,000; Piccoli et al., 1981);

	Geological Map of South Padova (1:50,000; Cucato et al., 2012).
Structural Map	Fantoni et al., 2002; Zampieri et al., 2003
Gravimetric Map	Ferri et al., 2005
Seismic sections	Pilli et al., 2012; Pola et al., 2014a
Deep wells	Final well logs (VIODEPI Project, https://www.videpi.com/)

4. Results

The sequence of hydrostratigraphic units (Fig. 3) from bottom to top is constituted by:

i. pre-Permian phyllites and micaschists;
ii. Permian clastic and evaporitic-carbonate rocks;
iii. Lower Triassic - Middle Triassic dolostones and limestones;
iv. Upper Triassic dolostones;
v. Lower Jurassic - Lower Cretaceous limestones;
vi. Lower Cretaceous - Eocene marly limestones;
vii. Eocene - Miocene clastic rocks locally intruded by Paleogene volcanic bodies;
viii. Quaternary cover, usually alluvial sediments.

In particular, the Upper Triassic dolostones and the Lower Jurassic – Lower Cretaceous limestones host the thermal aquifers.

The geometries of the main SVFS segments (SV, SC, TC, CP, and BV; Fig. 1) were established using seismic sections (Pola et al., 2014a). The faults dip at high angles toward the NE, showing dip variations up to 5° along the strike. A detailed representation of these variations would be computationally demanding and out of the scope of a regional reconstruction. Therefore, the faults were modeled using a constant dip (Table 3; Fig. 4a) reproducing their average dip value (Pola et al., 2014a).

The relay ramp, developed by the interaction of the SV and CP faults, was segmented by four main normal faults (R1, R2, R3 and R4; Fig. 1). Since seismic sections describing their geometries are lacking, the faults were modeled with constant dips of 85° (Table 3; Fig. 4a) reflecting the bounding fault dips.

The strike and geometries of the main Eastern Southern Alps thrusts (MA, PE and TB; Fig. 1) were reproduced on the basis of geological and structural maps and cross-sections (Antonelli et al., 1990; Pilli, 2012). Some simplifications were made during the reproduction of the thrusts. In particular, the Marana thrust and the Pedemontana thrust (MA and PE, respectively; Fig. 1) are segmented by minor subperpendicular faults. Although these local-scale faults are important in the geological characterization of the recharge area, they are not relevant for the regional groundwater flow. Consequently, they were reproduced as a single thrust (Fig. 4a).

After the reinterpretation of the geological sections using the proposed hydrostratigraphic sequence (Fig. 3) and their subsequent implementation into the MOVE software (Fig. 4b), the boundaries between the units were modeled. Figs. 4c and 4d show the bases of the Upper Triassic and Lower Cretaceous - Eocene hydrostratigraphic units corresponding to the bottom and top of the Euganean thermal reservoir, respectively. The aquifer is highly deformed in the northern part of the modeled area due to the Alpine multiphase compression (Fig. 4c). The base of the aquifer is locally jagged due to (i) the uplift of the underlying hydrostratigraphic units (not shown for better visualization), and (ii) the intersections with the topography. The units above the aquifer have been mostly eroded (only small portions remain in correspondence of the PE; Fig. 4d), allowing the direct infiltration of meteoric water into the aquifer. Moving toward the S, the most prominent deformation is the eastward deepening of the units accommodated by the regional and local faults. In this context, the faults of the interaction zone lift the units of the reservoir in the EuGF area, favoring the exploitation of the thermal waters at shallower depths (Fig. 5).

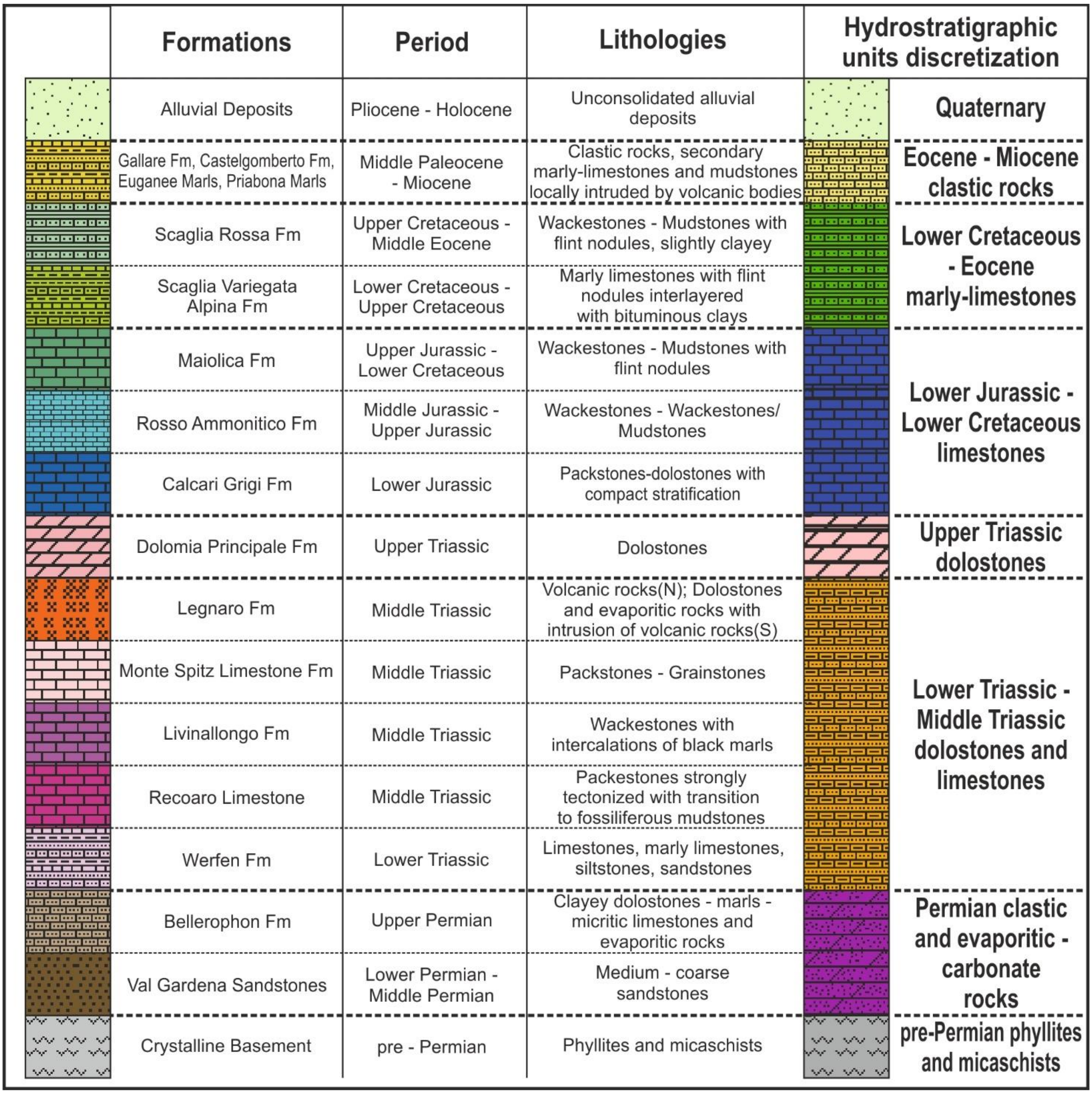

Fig. 3 Hydrostratigraphic units discretized from the stratigraphic sequence of the central Veneto region. Not to scale.

Table 2 Deep wells in the modeled area. The well locations are shown in Fig. 2.

Well Name	ID	Depth (m b.g.l.)	Perforation year	Type
Ballan 1	BA1	4,305	1987	Oil exploration
Codevigo 1	CD1	1,650	1987	Oil exploration
Legnaro 1	LE1	4,989	1973	Oil exploration
Metropole 1	ME1	1,044	2001	Thermal water exploitation
Sant'Angelo 1	SA1	2,036	1958	Oil exploration
Vicenza 1	VI1	2,150	1984	Oil exploration
Villadose 1	VD1	1,834	1957	Oil exploration
Villaverla 1	VL1	4,235	1978	Oil exploration

Table 3 SVFS faults (Fig. 1) and the dip angles and dip directions used for their reconstruction.

Fault Name	ID	Dip Angle	Dip Direction
Schio - Vicenza fault	SV	85°	NNE
Sandrigo - Camisano fault	SC	80°	NNE
Travettore - Codevigo fault	TC	85°	NNE
Conselve - Pomposa fault	CP	87°	NNE
Bovolenta fault	BV	70°	NNE
Realy Ramp 1 fault	R1	85°	NNW
Realy Ramp 2 fault	R2	85°	N
Realy Ramp 1 fault	R3	85°	NNE
Realy Ramp 1 fault	R4	85°	N

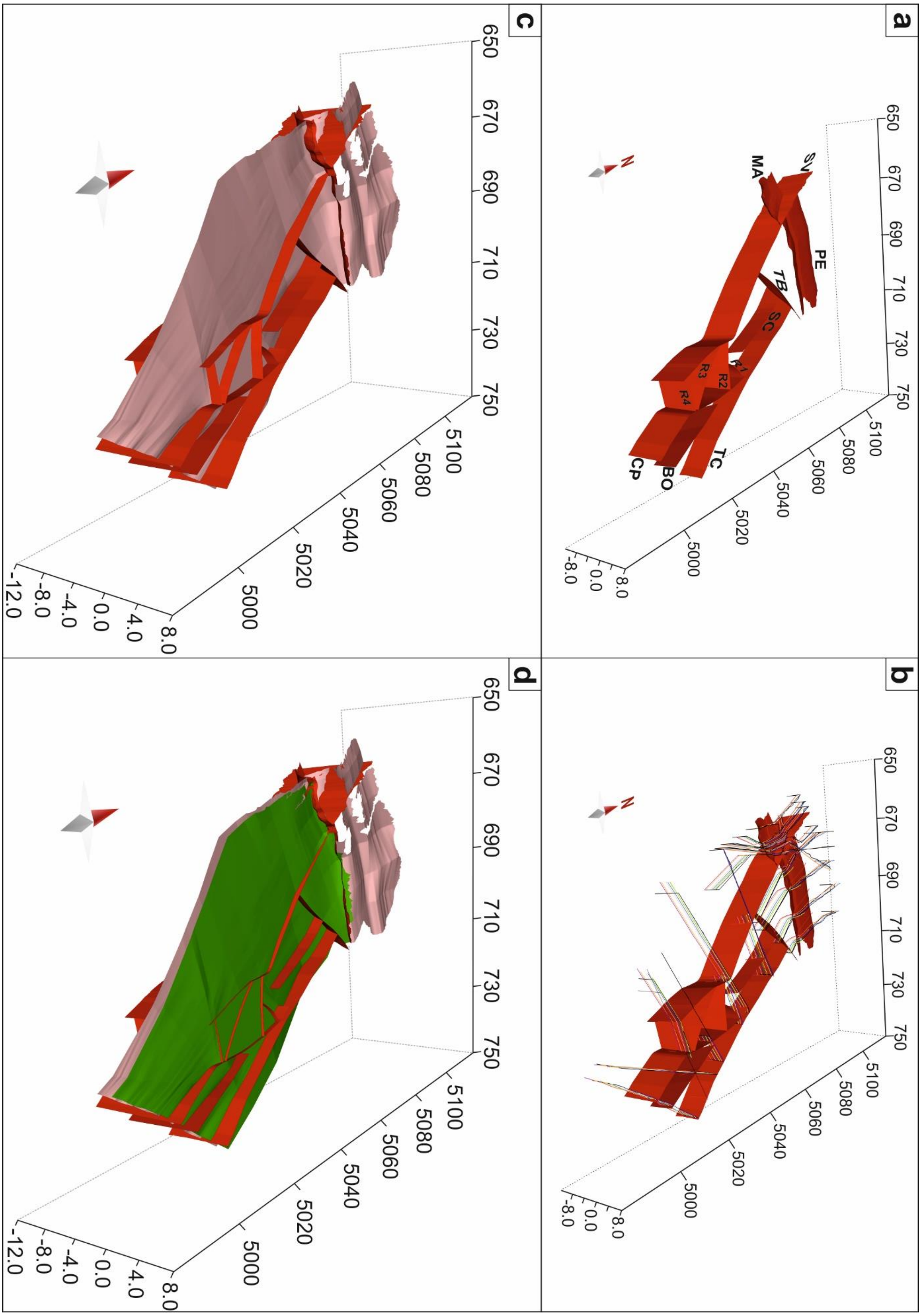

Fig. 4 3D hydrogeological reconstruction results. **(a)** Main regional fault modeling. The reader is referred to Fig. 1 for the acronyms of the faults. **(b)** Implementation of the geological sections. **(c)** Base of the Upper Triassic hydrostratigraphic

unit. **(d)**. Base of the Lower Cretaceous – Eocene hydrostratigraphic unit. Figs. **c** and **d** are vertically exaggerated (vertical exaggeration 2:1) to emphasize the structures

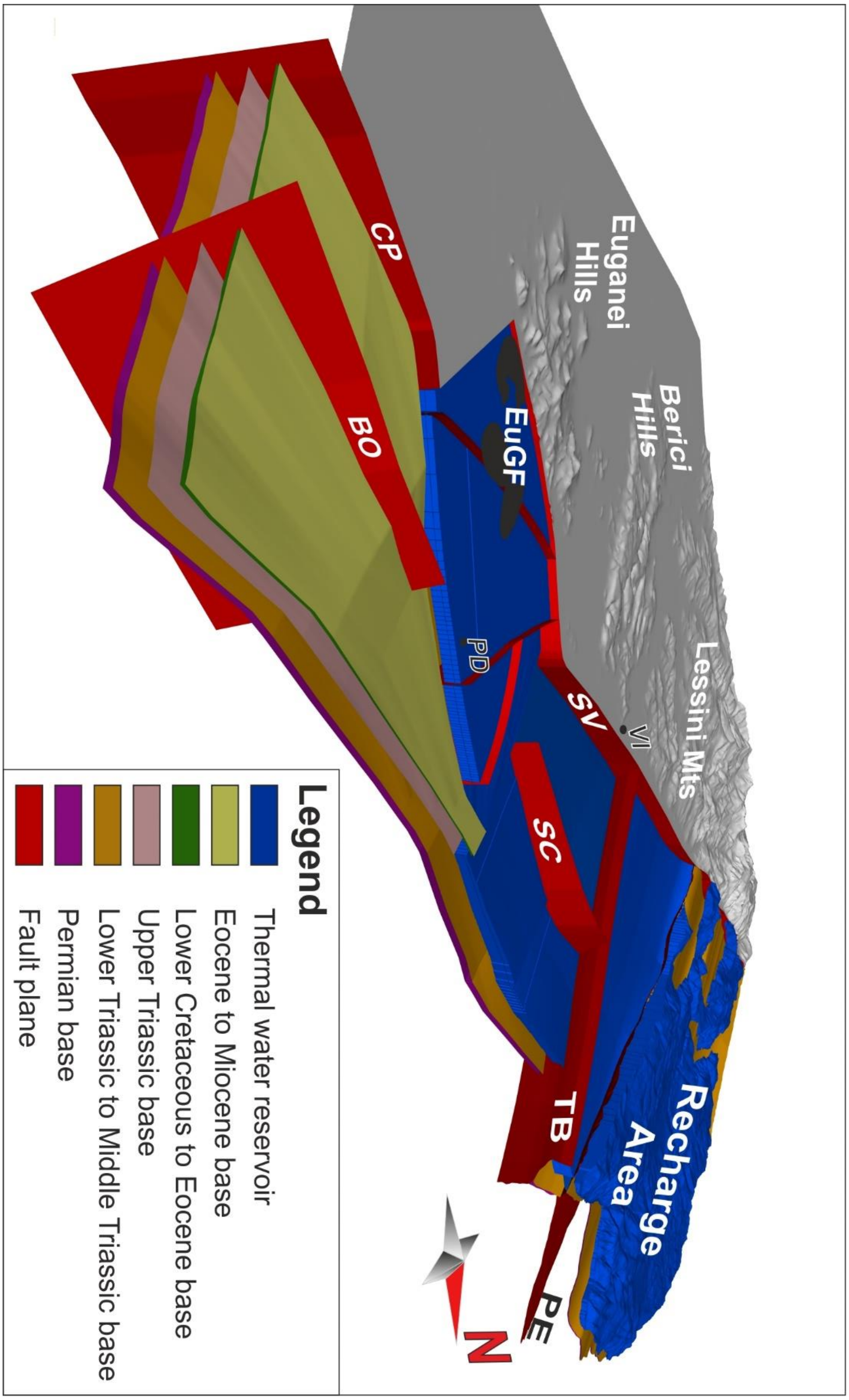

Fig. 5 3D hydrogeological reconstruction of the thermal reservoir (blue solid) extending from the Upper Triassic base to the Lower Cretaceous – Eocene base. The reader is referred to Fig. 1 for the acronyms of the faults.

5. Discussion

5.1 Model validation

The validation of the hydrogeological reconstruction was carried out by (i) deep well data for the Veneto plain area, and (ii) geological sections for the mountainous part of the study area (Fig. 6). These data were not used during the modeling phase. Two exploration wells (VD1 and CD1; Fig. 2) located close to the southern border of the model were excluded, since they intersect only the transition between the Quaternary alluvial cover and the Miocene-Eocene formations. In addition, considering that the EuGS is a fault-controlled geothermal system (Pola et al., 2014a; Zampieri et al., 2009), the hydrogeological reconstruction was performed and compared with literature information on the Veneto geological setting.

5.1.1 Validation of the Veneto plain area

A good correspondence is observed between the stratigraphic logs and the 3D reconstruction results (Fig. 7) and the discrepancies are generally lower than 150 m. In particular, the hydrogeological reconstruction shows good precision in the EuGF, as evidenced by the Metropole stratigraphic log (Fig. 6). The maximum discrepancies are 410 m for the Quaternary cover (Ballan 1 well) and 216 m for the rocky formations (Lower - Middle Triassic base in Villaverla 1 well). Considering the model thickness (9 km), variations lower than 270 m (approximately 3%) can be acceptable, since they are within the threshold that is generally accepted in hydrogeological numerical modeling (10%). The higher errors in the Quaternary reconstruction are related to both the local heterogeneities of this formation and the scarcity of the data, which does not allow a precise definition of such irregular lower limit of the unit. However, an approximate representation of the Quaternary base can be considered satisfactory since the EuGS develops into the bedrock.

A correlation between the hydrogeological reconstruction results and the stratigraphic logs was performed to enforce the achieved results. The bottoms depths (Fig. 8a) and the thicknesses (Fig. 8b) of each hydrostratigraphic unit were considered. A linear correlation with values of 0.99 and 0.83 for the depths and thicknesses, respectively, confirms the solidity of the performed hydrogeological reconstruction. The largest discrepancies are related to the Quaternary Formation and the Ballan well.

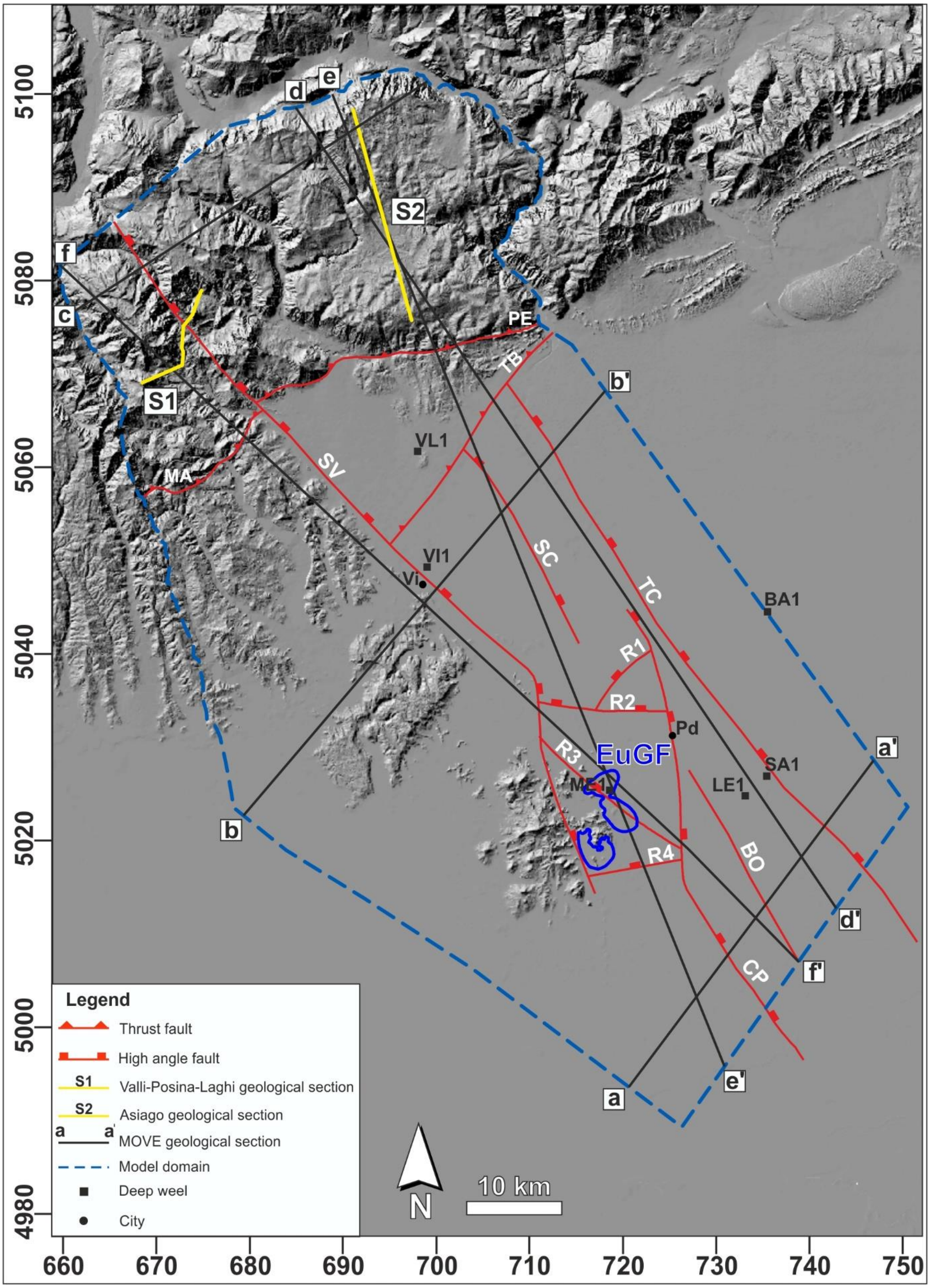

Fig. 6 Data used for the validation of the hydrogeological reconstruction. The reader is referred to Fig. 1 for the acronyms of the faults and cities and to Table 2 for the acronyms of wells. The coordinates are in the UTM zone 32N system using the WGS84 datum.

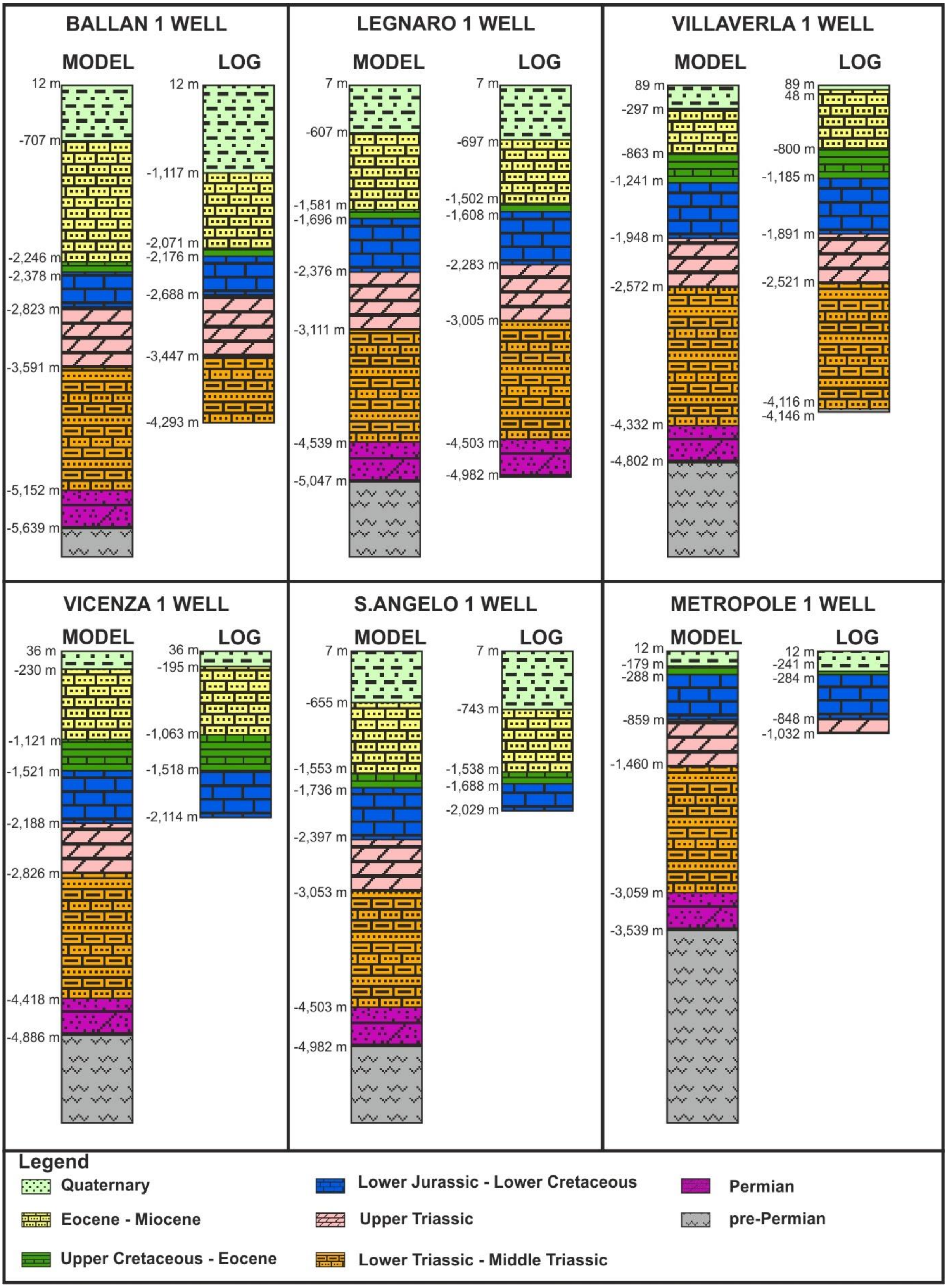

Fig. 7 Comparison between the stratigraphic logs of deep wells (Table 2) and the stratigraphic columns reconstructed from the model in the same locations. The well locations are shown in Fig. 2.

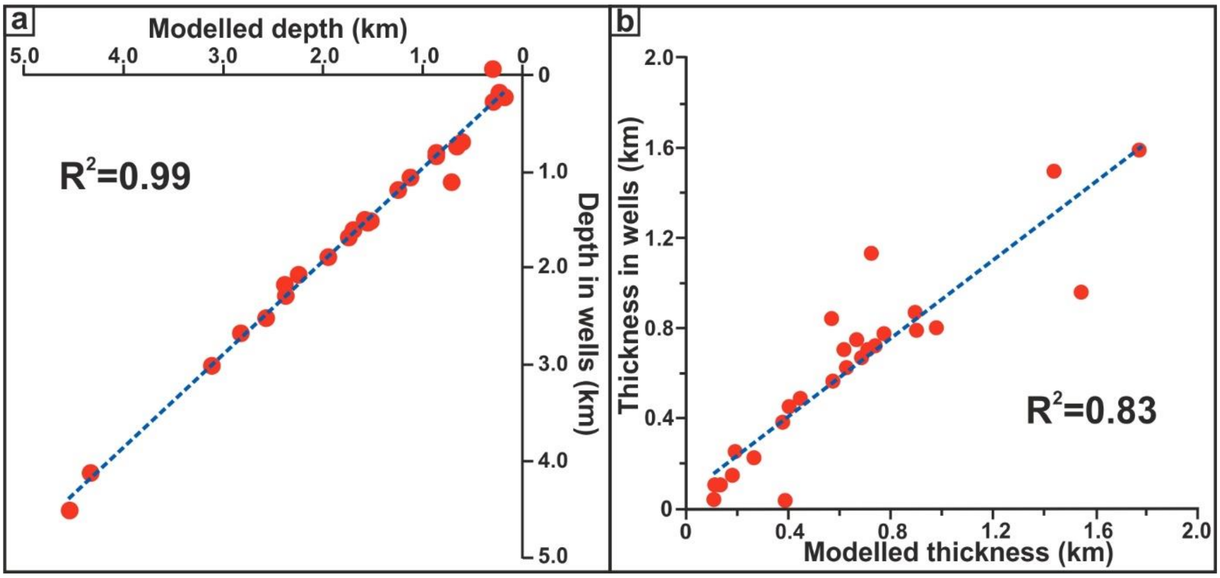

Fig. 8 Correlation between the depths of the hydrostratigraphic units bottoms obtained by the hydrogeological reconstruction and observed in the wells **(a)** and between the thicknesses of the hydrostratigraphic units in the reconstruction and in the wells **(b).**

5.1.2 Validation of the mountainous area

The S1 cross-section (Fig. 6) intersects the northern part of the SV fault and several local-scale faults (Fig. 9a; Sedea and Di Lallo, 1984) that were not reproduced into the reconstruction due to their minor impact on EuGS development. Fig. 9b represents the section that was modified according to the proposed discretization in hydrostratigraphic units. Where the sequence was incomplete, the section was extended considering (i) the thicknesses of the formations in the geological map, and (ii) the geometries of the outcropping horizons. The equivalent hydrostratigraphic section obtained from the hydrogeological reconstruction is shown in Fig. 9c. Generally, the geological setting is respected, and only minor differences in units thicknesses and geometries (i.e., folds) occur. The most relevant discrepancy is that the real throw of the SV fault is more prominent than the reconstruction (Fig. 9b and 9c, respectively). This observation will be detailed in the next paragraph.

The second geological section (S2; Fig. 6 and 10a; Barbieri and Grandesso, 2007) is located in the recharge area of the EuGS. Similar to S1, the minor faults with a secondary impact on the EuGS development were discarded, the section was reinterpreted using the hydrostratigraphic sequence and locally completed to intersect the crystalline basement (Fig. 10b). The section obtained from the hydrogeological reconstruction is shown in Fig. 10c. The model reproduces both the geometries of the units and their thicknesses well. The higher accuracy of this section than S1 is related to the lower heterogeneity of the geological setting in this sector of the Prealps.

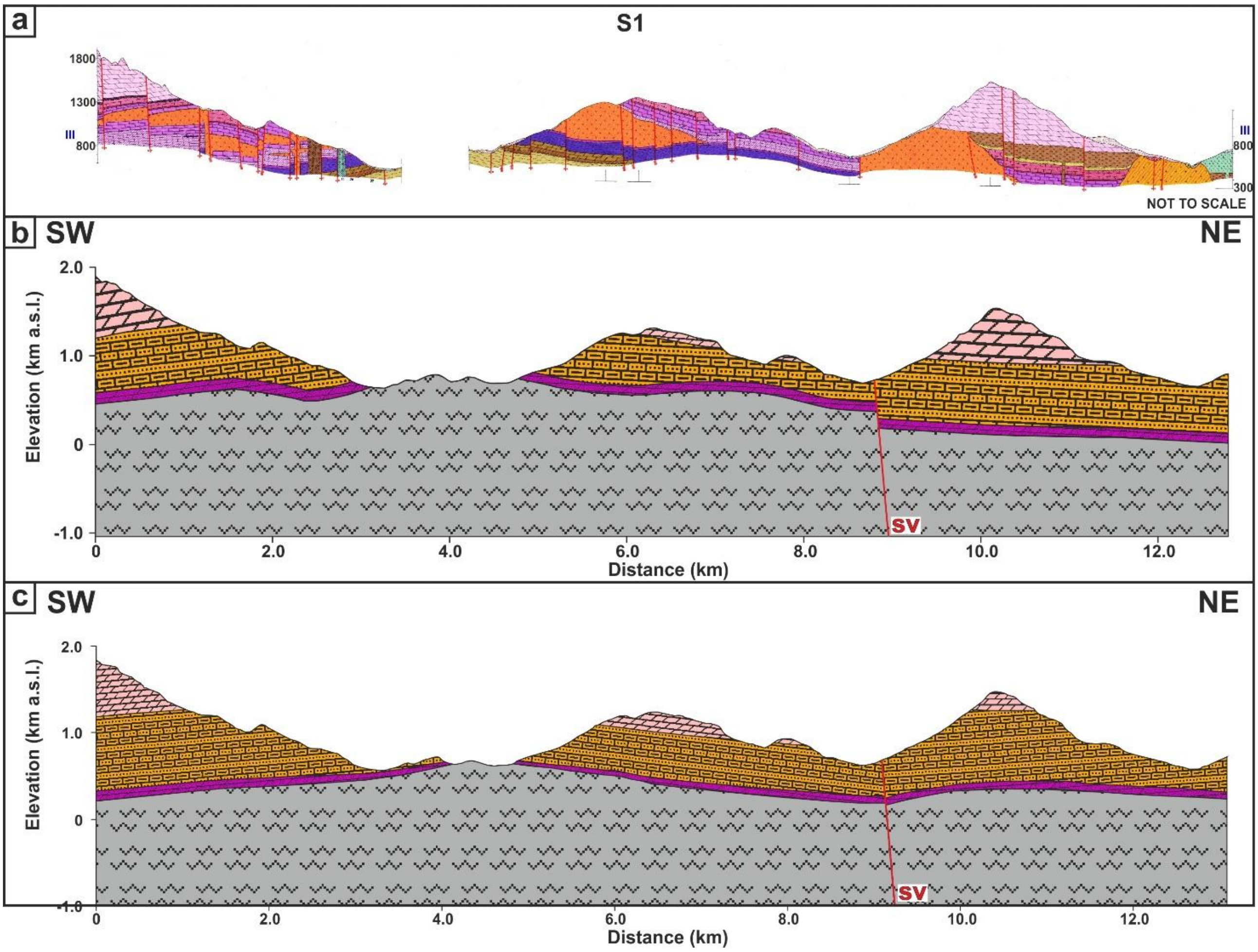

Fig. 9 (a). Geological cross-sections “III” in Sedea and Di Lallo, 1984 (not to scale). **(b)** Section modified using the hydrostratigraphic unit discretization. **(c)** Section obtained from the hydrogeological reconstruction. The reader is referred to Fig. 1 for the acronym of the fault and to Fig. 3 for the hydrostratigraphic unit colors.

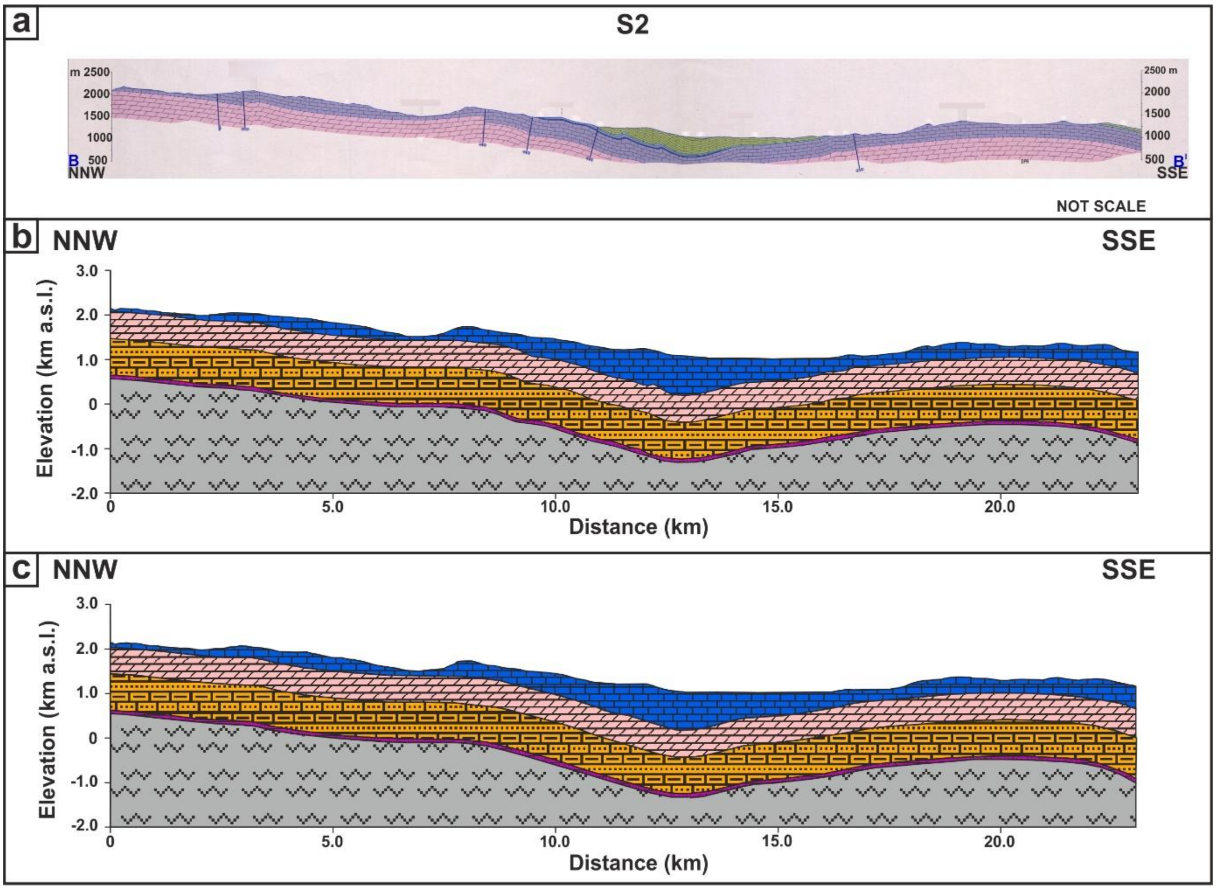

Fig. 10 (a) Geological cross-section "B-B'" in Barbieri and Grandesso, 2007 (not to scale). **(b)** Section modified using the hydrostratigraphic unit discretization. **(c)** Section obtained from the hydrogeological reconstruction. The reader is referred to Fig. 1 for the acronym of the fault and to Fig. 3 for the hydrostratigraphic unit colors.

5.1.3 Structural setting validation

The structural setting reproduced by the hydrogeological reconstruction was analyzed through four cross-sections (Figs. 6 and 11) and discussed in relation to the structural interpretation of the central Veneto region.

Analyzing Fig. 11a and Fig. 11b, the eastward deepening of the bedrock from the LBE block to the Veneto plain foredeep is determined by the SVFS. The increase in the thickness of the Mesozoic Formation (approximately 1 km) moving from W to E indicates that the SVFS activity occurred during the Mesozoic extensional phase (Pola et al., 2014a). Moving from the footwall of the SV fault to the hanging wall of the TC fault, an increased thickness of approximately 1.7 km in the Eocene – Miocene unit is observed. This finding is related to the deep sedimentary basin developed in the eastern part of the Veneto-Friuli foredeep (east of the model domain), whose deformation in the study area is less pronounced and is associated with the Alps loading during the Chattian-Langhian flexure cycle (Fantoni et al., 2002).

Fig. 11d shows a northward and southward inflection of the Veneto foredeep bedrock formations. The first inflection, affecting the bedrock formation south of the TB thrust, is related to two different flexure cycles: (i) the Chattian-Langhian cycle seen before, and (ii) the Serravallian-Lower Messinian cycle characterized by prominent flexure associated with the build-up of the Eastern Southern Alps (Fantoni et al., 2002; Zattin et al., 2006). On the other hand, the southward inflection is correlated to the pre-Early Pliocene flexure as a consequence of the build-up of the North Apennines (Brancolini et al., 2019; Fantoni et al., 2002).

Moving to the northernmost part of the model domain, there is a change in the dip separation of the SV fault varying from normal to reverse (sections b-b' in Fig. 11a and c-c' in Fig. 11c, respectively). This change is apparent and can be explained considering the evolution of the Eastern Southern Alps. The Pedemontana thrust has determined the uplift of the northern sector to be approximately 1 km (Pellegrini, 1988). In addition, Castellarin and Cantelli (2000) determined that the amplitude of the folds in the NE sector of the SV fault is greater than the amplitude of the folds in the SW sector. Consequently, the apparent change in kinematics along the SV fault is correlated to the Pedemontana thrust action, which determined the uplift of the SV hanging wall in the mountain area compared to that of the SV footwall.

5.2 Conceptual model validation

The 3D hydrogeological reconstruction was used to validate the EuGS hydrogeological conceptual model. A N-S cross-section (Fig. 11e) was performed through the recharge and the exploitation areas. The hypothesized recharge area of the Sette Comuni and Tonezza plateaus is located at a mean elevation of approximately 1,500 m a.s.l., which is in agreement with the isotopic composition of the thermal water (Gherardi et al., 2000). This area is affected by both a high degree of fracturing related to local-scale faults and a well-developed karst system. These features increase the local permeability of the Mesozoic outcropping rocks, favoring the infiltration of meteoric waters. Moving toward the S, a progressive deepening of the rocky formations occurs. In the sector between the TB and R2 faults (hanging wall of the Schio-Vicenza fault), the thermal water reservoir units show depths between approximately 1.2 and 1.7 km (top of the reservoir) and between 2.3 and 3 km (bottom of the reservoir; Fig. 11e). Gherardi et al. (2000) hypothesized that the Euganean thermal water had a groundwater circulation depth of 2.5-3 km, which was estimated from the SiO_2 and K/Mg geothermometer results and assuming a normal geothermal gradient of 30 °C/km. However, the slightly anomalous crustal heat flow characterizing the central Veneto region (Pasquale et al., 2014) and the consequent anomalous geothermal gradient could produce the same temperature values at shallower depths as observed in the hanging wall of the SV (Fig. 11e). To the S, the high-angle faults of the relay ramp determine the rise of the hydrostratigraphic sequence. The thermal reservoir is at depths between 0.3 km (top of the reservoir) and 1.5 km (bottom of the reservoir), in accordance with the depth of the EuGF thermal wells (0.3 - 1 km).

From a general perspective, it is important to highlight that the main regional faults, i.e., NW-dipping thrust and SVFS, and the local-scale structures, i.e., relay ramp, permit the geological continuity of the thermal aquifer from the recharge area to the exploitation field. In the recharge area, the aquifer outcrops favoring the infiltration of meteoric waters. The altitude of the recharge area provides hydrostatic pressure to the meteoric waters, developing a topographically driven regional groundwater flow. The regional faults and their damage zones locally enhance the regional fluid flow. In particular, the damage zone of the SV fault could be the widest and most permeable, considering the correlation between fault slip and damage zone thickness (Savage and Brodsky, 2011). The damage zone could be composed of a complete set of Riedel-type faults and fractures, as observed in the synthetic sinistral faults deforming the eastern margin of the Lessini Mountains and Berici Hills. In the Euganean area, the regional deformation is accommodated by the relay ramp and its result is the rise of thermal aquifers at depths shallower than the surrounding area of the Veneto plain block. The intense deformation within this structure increases the local permeability field, favoring the regional to local fluid flow, the local convection, and the rising and discharge of the thermal waters. The numerical simulation results based on a schematic representation of the Euganean Geothermal System quantified the importance of these processes in developing the EuGF (Pola et al., 2020). Furthermore, the relay ramps are favorable structures for the development of thermal anomalies, as observed in worldwide geothermal systems (Faulds et al., 2013; Fossen and Rotevatn, 2016; Rotevatn and Peacock, 2018; Rowland and Sibson, 2004).

The early studies on the EuGS (Piccoli et al., 1976) suggested that the thermal waters infiltrate into the Piccole Dolomiti and Lessini mountains west of the SV fault (Fig. 1a). This hypothesis was discarded by Pola et al. (2015b), and the recharge area was moved east of the SV fault into the Tonezza and Sette Comuni plateaus. This change was based on the analysis of the local geological settings of these areas. In fact, section f-f' (Fig. 11f) shows that the dolomite formations cropping into the Piccole Dolomiti Mountains are separated from the Mesozoic carbonates of the thermal reservoir in the subsurface of the Lessini Mountains by the pre-Permian crystalline basement. The basement can be considered impervious (hydraulic conductivity of 10^{-10} m/s measured in a core sample from a deep well), inhibiting the southward flux of the infiltrated meteoric waters. Only the carbonates between the pre-Permian basement and the Marana thrust (Fig. 1b; Fig. 11f) could be a possible recharge zone. However, this hypothesis is unlikely, since (i) the mean altitude of this area is lower than the infiltration altitude as suggested by the stable isotope contents of the waters, and (ii) its extent is relatively small and doesn’t guarantee the adequate feeding to the system for maintaining the potentiometric level in the EuGF related to the current exploitation. This area could be considered as an additional portion of the recharge area by either slightly contributing to the EuGS or feeding local subthermal circulation systems in the Lessini and Berici mountains.

5.3 Reservoir volume and thermal water resource estimation

The 3D hydrogeological reconstruction was used to estimate the volume of the thermal reservoir. Although there are two aquifer layers exploited in the EuGF, they can be considered as one body at the regional scale. First, the calculation was performed in the area affected by the thermal water circulation that extends from the recharge area to the fault interaction zone. Afterwards, the Lessini-Berici-Euganei undeformed foreland and the hanging walls of the Travettore-Codevigo and Conselve-Pomposa faults were excluded. The volume obtained (V_{total}; Fig. 5) was 1.91x 10^{12} m^3. The amount of groundwater into the reservoir (V_{eff}) was estimated using the literature values of n_e for the reservoir lithologies (Pasquale et al., 2011). The results achieved by the three considered scenarios of n_e are summarized in Table 4.

Subsequently, a comparison between the calculated (V_{eff}) and the exploited (V_{exp}) volumes of water was performed to estimate the impact of human activities on the system. For this purpose, the EuGS can be considered a closed system, since (i) the waters have a long residence time (approximately several thousand years; Gherardi et al., 2000), and (ii) the exploitation period is relatively short compared with the long lifespan of the system (approximately 150 years and more than 30±4 ka, respectively; Fabbri et al., 2017; Pola et al., 2014b). Consequently, the total exploitation in the 20th and 21st centuries was calculated, while the outflow of thermal springs was neglected, since their flow rate was much smaller than the forced extraction and could be considered to be in secular equilibrium with the system recharge. The amount of thermal water exploited to date is approximately 1.18 x 10^9 m^3 (Fabbri et al., 2017), representing a small percentage of the groundwater in the regional reservoir (V_{exp}/V_{eff} in Table 4).

Since the geothermal manifestation occurs only in the relay ramp, the volume calculation was limited to (i) the interaction zone and (ii) the EuGF area. The reservoir volumes (V_{total}) were 2.41 x 10^{11} m^3 and 1.04 x 10^{10} m^3, respectively. Considering the groundwater volume in the interaction zone (V_{eff} in Table 4), the anthropogenic impact is more evident than in the regional scenario. In fact, the exploited volumes are between 6% and 50% of the effective volume of the reservoir. By reducing the size of the reservoir at the EuGF scale, an overexploitation is shown in all three scenarios of n_e (Table 4).

In terms of the Euganean thermal resource management, Table 4 shows that the amount of groundwater at the regional scale is very high compared to the overall exploited volume. This result could indicate the possibility of increasing the rate of annual exploitation in the EuGF area, which is currently 15 x 10^6 m^3/y. However, this assumption is in contrast with the decrease in the potentiometric level during the 1960s and 1970s that was caused by an overexploitation of the system (20 - 28 x 10^6 m^3/y) and resulted in the Euganean thermal springs drying up (Fabbri et al., 2017). The overestimate in the regional scenario is caused by the fact that the real flow paths within the system are not considered and the whole volume of the Upper Triassic and Lower Jurassic-Lower Cretaceous units in the central part of the modeled area is accounted for feeding the EuGF. However, the role of the regional fault damage zones in enhancing the regional fluid flow would be difficult to properly quantify, since their real extent and hydrogeological properties are not known. Similarly, excluding the fracturing and the available values of the Euganean aquifer hydrogeological properties suggests a severe overexploitation in the EuGF scenario. This is probably unrealistic considering that exploitation was minimal in the first half of the 20th century and that a balance between exploitation and thermal water recharge has been recently achieved.

The results obtained from this preliminary volume estimation confirm that the amount of groundwater into the system is sufficient compared with the exploited volume. However, a management plan for the sustainable exploitation of Euganean thermal water should include also the hydraulic features of the system, the groundwater flow paths, and the portion of reservoirs affected by exploitation. The use of numerical simulations supported by a realistic representation of the hydrogeological system can be a helpful tool to evaluate the impact of exploitation on the resource for its long-lasting preservation.

Table 4 Estimation of the available groundwater volume in the Euganean reservoir. V_{total}: total volume of the reservoir; V_{eff}: effective volume of groundwater into the reservoir; V_{exp}: total volume of exploited thermal waters; V_{exp}/V_{eff}: percentage of exploited waters with respect to groundwaters available into the reservoir.

		Effective porosity [%]	V_{total} [m^3]	V_{eff} [m^3]	V_{exp} [m^3]	V_{exp}/V_{eff} [%]
EuGS	Maximum	8	1.91×10^{12}	1.53×10^{11}	1.18×10^{9}	0.8
	Mean	4	1.91×10^{12}	7.64×10^{10}	1.18×10^{9}	1.5
	Minimum	1	1.91×10^{12}	1.91×10^{10}	1.18×10^{9}	6.1
Interaction zone	Maximum	8	2.41×10^{11}	1.93×10^{10}	1.18×10^{9}	6.2
	Mean	4	2.41×10^{11}	9.63×10^{9}	1.18×10^{9}	12.3
	Minimum	1	2.41×10^{11}	2.41×10^{9}	1.18×10^{9}	49.2
EuGF	Maximum	8	1.04×10^{10}	8.31×10^{8}	1.18×10^{9}	142.5
	Mean	4	1.04×10^{10}	4.16×10^{8}	1.18×10^{9}	284.9
	Minimum	1	1.04×10^{10}	1.04×10^{8}	1.18×10^{9}	1,139.7

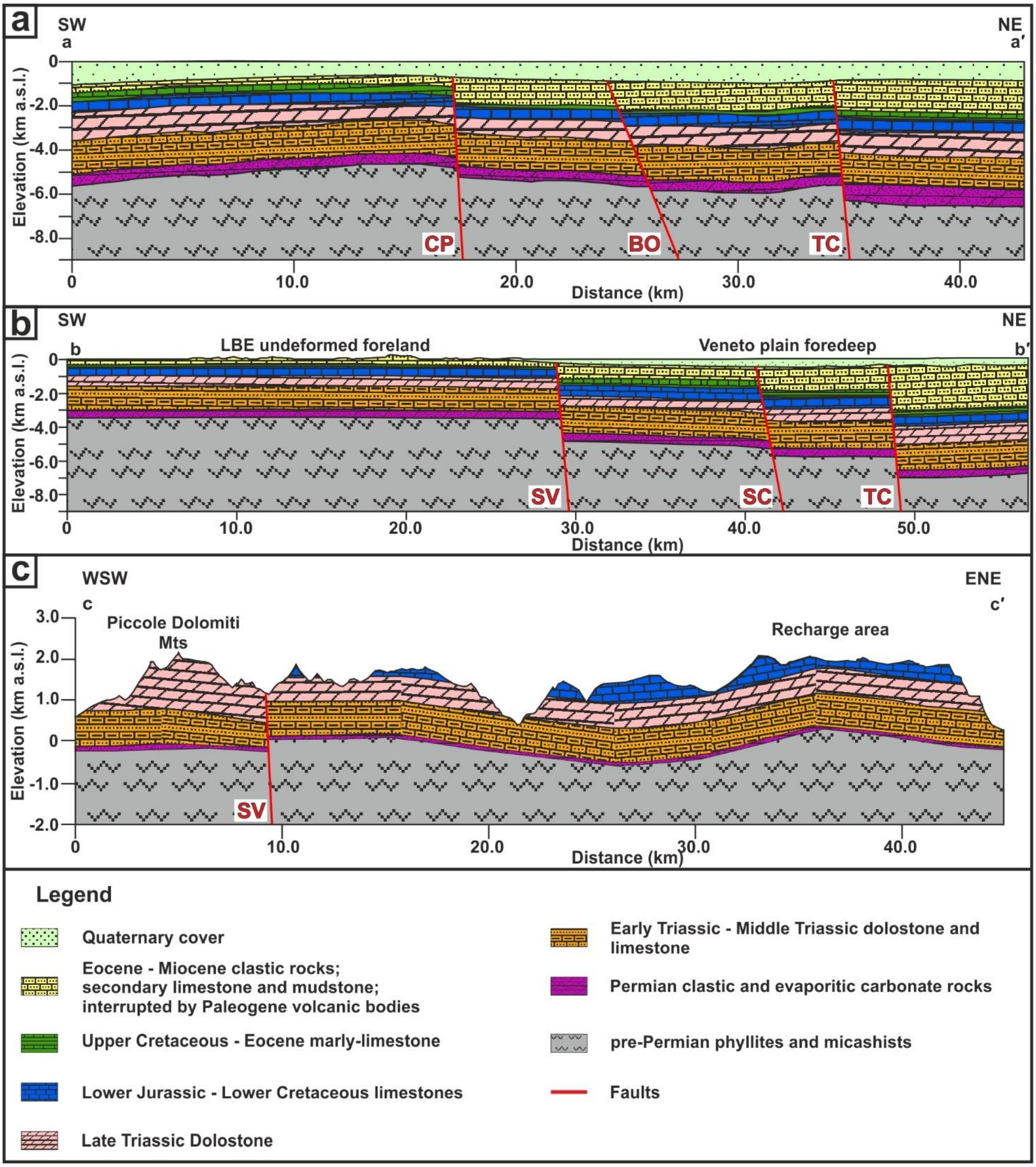

a
SW
a
NE
a′
Elevation (km a.s.l.)
0
-2.0
-4.0
-6.0
-8.0
CP
BO
TC
0
10.0
20.0
30.0
40.0
Distance (km)
b
SW
NE
b
b′
LBE undeformed foreland
Veneto plain foredeep
Elevation (km a.s.l.)
SV
SC
TC
50.0
Distance (km)
c
WSW
ENE
c
c′
Piccole Dolomiti
Mts
Recharge area
3.0
2.0
1.0
-1.0
-2.0
SV
Distance (km)
Legend
Quaternary cover
Eocene - Miocene clastic rocks;
secondary limestone and mudstone;
interrupted by Paleogene volcanic bodies
Upper Cretaceous - Eocene marly-limestone
Lower Jurassic - Lower Cretaceous limestones
Late Triassic Dolostone
Early Triassic - Middle Triassic dolostone and
limestone
Permian clastic and evaporitic carbonate rocks
pre-Permian phyllites and micashists
Faults

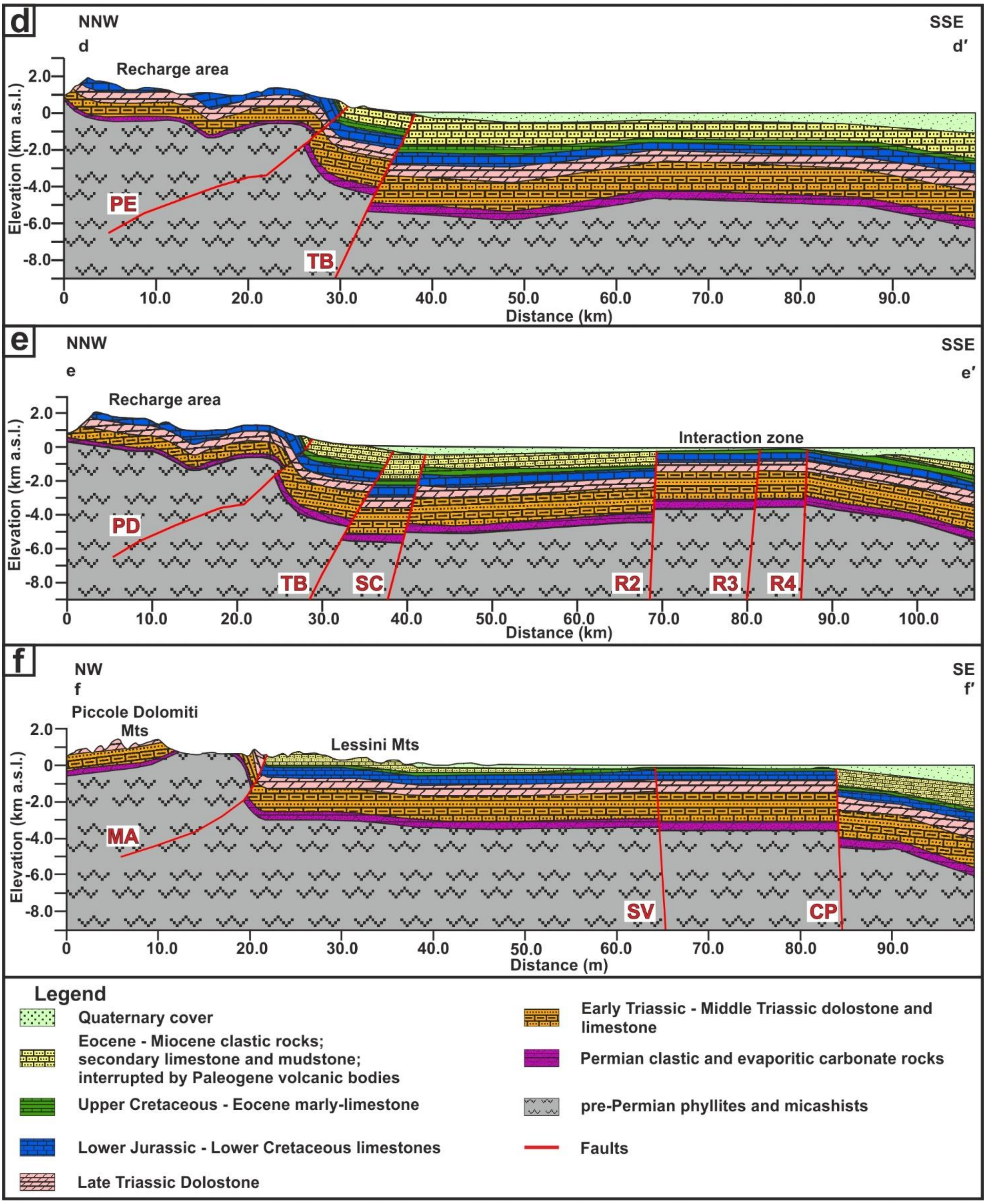

Fig. 11 a SW – NE oriented section located in the southern part of the domain. **b** SW – NE oriented section located in the central part of the domain. **c** WSW – ENE oriented section located in the northern part of the domain. Vertical exaggeration 2:1; **d** NNW – SSE oriented section. Vertical exaggeration 2:1; **e** NNW – SSE oriented section. Vertical exaggeration 2:1; **f** NW – SE oriented section. Vertical exaggeration 2:1. The reader is referred to Fig. 1 for the acronyms of the faults.

6. Conclusions

In this study, the 3D hydrogeological reconstruction of the fault-controlled Euganean Geothermal System (EuGS) was presented. The aims of this work were (i) to evaluate the role of the main regional faults on the development of the EuGS; (ii) to validate the EuGS hydrogeological conceptual model, and (iii) to estimate the thermal water volumes in the reservoir in comparison with the exploited volume in the last 100 years. Gravimetric, structural, and geological maps and geological cross-sections were used to perform the hydrogeological reconstruction. The geological sequence of the central part of the Veneto region was discretized into 8 hydrostratigraphic units on the basis of their hydrogeological behavior and their role in the development of the geothermal system. The reconstruction was performed and validated through the stratigraphic logs of deep boreholes and cross-sections. The cross-sections construed from this reconstruction elucidated the relationship between the regional and local structures and the groundwater flow. An estimation of the groundwater volumes into the EuGS was performed at different scales and considering three possible scenarios of effective porosity. Because the local hydraulic parameters of the EuGF and the groundwater flow paths were not considered, the analyses provide only an approximate estimate of the available thermal water volumes. However, the combination of these results with numerical simulations based on the hydrogeological reconstruction results will be a helpful instrument to quantify the renewability of the Euganean resource and to assess a management plan for its sustainable exploitation.

Although in the proposed work the hydrogeological reconstruction was employed to increase the knowledge of a geothermal system, the same approach can be profitably used to study other geological and hydrogeological systems in which the geological setting and the structural features play a fundamental role in their development.

A detailed 3D subsurface geology modeling can be profitable used to several purposes, such as: (i) numerical model implementation adopting a geological-base model domain; (ii) validation of the available geological data through their implementation into a 3D workspace; (iii) validation of the geological/hydrogeological conceptual model that explains the development of a phenomenon; (iv) quantify the size of geological and structural elements in terms of volume, areal extension, etc., and (v) to evaluate the interrelationship between geological and structural features and individuate the critical/peculiar sectors of the analyzed system (i.e. recharge area, contaminant source, reservoir location, etc.)

Acknowledgments

The authors would like to thanks the Editors and two anonymous Reviewers for their revisions and constructive comments which greatly improved this manuscript.

Funding

This researcher was funded by the hydrothermal district of Euganean Geothermal Field (B.I.O.C.E.) within the project “Hydrogeological model of Euganean Geothermal System (EuGS)”, grant to P. Fabbri.

7. Data Availability

Dataset related to this article can be found at http://researchdata.cab.unipd.it/id/eprint/329 an open-source online data repository.

8. References

Antonelli, R., Barbieri, G., Dal Piaz, G.V., Dal Pra, A., De Zanche, V., Grandesso, P., Mietto, P., Sedea, R., Zanferrari, A., 1990. Carta Geologica del Veneto 1:250,000 e relative Note Illustrative. S.E.L.C.A., Firenze.

Aurighi, M., Cisotto, A., Dal Prá, A., Janza, M., Mariani, R., Nordico, M., Soccorso, C., Steccanella, D., Barbieri, G., 2004. Carta idrogeologica dell'Altopiano dei Sette Comuni. Regione Veneto, Giunta Regionale, 31 pp

Axelsson, G., 2010. Sustainable geothermal utilization - Case histories; definitions; research issues and modelling. Geothermics 39, 283–291. https://doi.org/10.1016/j.geothermics.2010.08.001

Barbieri, G., De Zanche, V., Di Lallo, E., Mietto, P., Sedea, R., 1980. Carta Geologica dell'area di Recoaro 1:20,000. Litografia artistica e cartografica, Firenze.

Barbieri, G., Grandesso, P., 2007. Note Illustrative Della Carta Geologica D'Italia Alla Scala 1:50,000, Foglio 82 Asiago. ISPRA, 135pp

Bartoli, O., Meli, S., Bergomi, M.A., Sassi, R., Magaraci, D., Liu, D.Y., 2015. Geochemistry and zircon U-Pb geochronology of magmatic enclaves in trachytes from the Euganean Hills (NE Italy): further constraints on Oligocene magmatism in the eastern Southern Alps. Eur. J. Mineral. 27, 161–174. https://doi.org/10.1127/ejm/2015/0027-2425

Bellieni, G., Fioretti, A.M., Marzoli, A., Visonà, D., 2010. Permo-Paleogene magmatism in the eastern Alps. Rend. Lincei 21, 51–71. https://doi.org/10.1007/s12210-010-0095-z

Blöcher, M.G., Cacace, M., Lewerenz, B., Zimmermann, G., 2010. Three dimensional modelling of fractured and faulted reservoirs: Framework and implementation. Chemie der Erde 70, 145–153. https://doi.org/10.1016/j.chemer.2010.05.014

Brancolini, G., Civile, D., Donda, F., Tosi, L., Zecchin, M., Volpi, V., Rossi, G., Sandron, D., ferrante, G. M., Forlin, E., 2019. New insights on the Adria plate geodynamics from the northern Adriatic perspective. Marine and Petroleum Geology, https://doi.org/10.1016/j.marpetgeo.2019.06.049

Cacace, M., Blöcher, G., 2015. MeshIt—a software for three dimensional volumetric meshing of complex faulted reservoirs. Environ. Earth Sci. 74, 5191–5209. https://doi.org/10.1007/s12665-015-4537-x

Castellarin, A., Cantelli, L., 2000. Neo-Alpine evolution of the Southern Eastern Alps. J. Geodyn. 30, 1–2. https://doi.org/10.1016/S0264-3707(99)00036-8

Cataldi, R., 2001. Sustainability and renewability of geothermal energy. In: Inter- national Scientific Conference on Geothermal Energy in Underground Mines, Ustron, Poland, 4 pp.

Consorzio Terme Euganee, 2016. Thermae Abano Montegrotto −Momenti Da Vivere. Consorzio Terme Euganee, Abano Terme. http://www.consorziotermeeuganee.it/ attivita/ufficio-stampa/.

Cucato, M., De Vecchi, G.P., Mozzi, P., Abbà, T., Paiero, G., Sedea, R., et al., 2012. Note Illustrative Della Carta Geologica D'Italia Alla Scala 1:50,000, Foglio 147 Padova Sud. ISPRA, 215pp.

Cushing, E.M., Hollender, F., Moiriat, D., Guyonnet-Benaize, C., Theodoulidis, N., Pons-Branchu, E., Sépulcre, S., Bard, P.Y., Cornou, C., Dechamp, A., Mariscal, A., Roumelioti, Z., 2020. Building a three dimensional model of the active Plio-Quaternary basin of Argostoli (Cephalonia Island, Greece): An integrated geophysical and geological approach. Eng. Geol. 265, 105441. https://doi.org/10.1016/j.enggeo.2019.105441

De Vecchi, G.P., Sedea, R., 1983. Il vulcanismo medio-Triassico nelle Prealpi vicentine (Italia settentrionale). Mem. Sci Geol., 36, 149-169.

De Vecchi, G.P., Sedea, R., 1995. The Paleogene basalts of the Veneto region (NE Italy). Mem. Sci Geol., 47, 253-274.

Diaz, A.R., Kaya, E., Zarrouk, S.J., 2016. Reinjection in geothermal fields − A worldwide review update. Renewable and Sustainable Energy Review 53, 105-162. https://doi.org/10.1016/j.rser.2015.07.151.

Fabbri, P., 1997. Transmissivity in the Geothermal Euganean Basin: A Geostatistical Analysis. Ground Water. https://doi.org/10.1111/j.1745-6584.1997.tb00156.x

Fabbri, P. (2001). Probabilistic assessment of temperature in the Euganean geothermal area (Veneto region, NE Italy). Mathematical Geology, 33(6), 745–760. https://doi.org/10.1023/A:1011030900322

Fabbri, P., Trevisani, S. (2005). Spatial distribution of temperature in the low-temperature geothermal Euganean field (NE Italy): A simulated annealing approach. Geothermics, 34(5), 617–631. https://doi.org/10.1016/j.geothermics.2005.07.001

Fabbri, P., Pola, M., Piccinini, L., Zampieri, D., Roghel, A., Dalla, N., 2017. Monitoring, utilization and sustainable development of a low-temperature geothermal resource: A case study of the Euganean Geothermal Field (NE, Italy). Geothermics 70, 281–294. https://doi.org/10.1016/j.geothermics.2017.07.002

Fantoni, R., Catellani, D., Merlini, S., Rogledi, S., Venturini, S., 2002. La registrazione degli eventi deformativi cenozoici nell’avampaese Veneto-Friulano. Mem. della Soc. Geol. Ital. 57, 301–313.

Faulds, J.E., Hinz, N.H., Dering, G.M., Siler, D.L., 2013. The Hybrid Model — The Most Accommodating Structural Setting for Geothermal Power Generation in the Great Basin, Western USA. Geothermal Resources Council Transactions 37, 4–10.

Ferri, F., Ventura, R., Coren, F., Zanolla, C., 2005. Gravity Map of Italy and Surroundings Seas 1:1250000. — APAT Agenzia per la protezione dell’ambiente e per i servizi tecnici. Dipartimento Difesa del Suolo, 15 p.

Fossen, H., Rotevatn, A., 2016. Fault linkage and relay structures in extensional settings-A review. Earth-Science Rev. 154, 14–28. https://doi.org/10.1016/j.earscirev.2015.11.014

Franco, A., Vaccaro, M., 2014. Numerical simulation of geothermal reservoirs for the sustainable design of energy plants: A review. Renew. Sustain. Energy Rev. 30, 987–1002. https://doi.org/10.1016/j.rser.2013.11.041

Gherardi, F., Panichi, C., Caliro, S., Magro, G., Pennisi, M., 2000. Water and gas geochemistry of the Euganean and Berician thermal district (Italy). Appl. Geochemistry 15, 455–474. https://doi.org/10.1016/S0883-2927(99)00056-6

Ghiglieri, G., Carletti, A., Da Pelo, S., Cocco, F., Funedda, A., Loi, A., Manta, F., Pittalis, D., 2016. Three-dimensional hydrogeological reconstruction based on geological depositional model: A case study from the coastal plain of Arborea (Sardinia, Italy). Eng. Geol. 207, 103–114. https://doi.org/10.1016/j.enggeo.2016.04.014

Hassen, I., Gibson, H., Hamzaoui-Azaza, F., Negro, F., Rachid, K., Bouhlila, R., 2016. 3D geological modeling of the Kasserine Aquifer System, Central Tunisia: New insights into aquifer-geometry and interconnections for a better assessment of groundwater resources. J. Hydrol. 539, 223–236. https://doi.org/10.1016/j.jhydrol.2016.05.034

Hill, D.P., 1977. A model for earthquake swarms. J. Geophys. Res. 82, 1347–1352. https://doi.org/10.1029/JB082i008p01347

Høyer, A.S., Klint, K.E.S., Fiandaca, G., Maurya, P.K., Christiansen, A. V., Balbarini, N., Bjerg, P.L., Hansen, T.B., Møller, I., 2019. Development of a high-resolution 3D geological model for landfill leachate risk assessment. Eng. Geol. 249, 45–59. https://doi.org/10.1016/j.enggeo.2018.12.015

Huenges, E., 2010. Geothermal Energy Systems – Exploration Development And Utilization. Weinheim: Wiley-VCH, 463pp.

Ingebritsen, S.E., Geiger, S., Hurwitz, S., Driesner, T., 2010. Numerical simulation of magmatic hydrothermal systems - Ingebritsen - 2010 - Reviews of Geophysics 48, RG1002, doi:10.1029/2009RG000287.

International Energy Agency, 2019. World Energy Outlook 2019. OECD/IEA, Paris.

Kaya, E., Zarrouk, S., O'Sullivan, M., 2011. Reinjection in geothermal fields – a review of worldwide experience. Renew Sustain Energy Rev 15, 47–68. https://doi.org/10.1016/j.rser.2010.07.032

Limberger, J., Boxem, T., Pluymaekers, M., Bruhn, D., Manzella, A., Calcagno, P., Beekman, F., Cloetingh, S., van Wees, J.D., 2018. Geothermal energy in deep aquifers: A global assessment of the resource base for direct heat utilization. Renew. Sustain. Energy Rev. 82, 961–975. https://doi.org/10.1016/j.rser.2017.09.084

Lund, J.W., Boyd, T.L., 2016. Direct utilization of geothermal energy 2015 worldwide review. Geothermics 60, 66–93. https://doi.org/10.1016/j.geothermics.2015.11.004

Mantovani, E., Babbucci, D., Tamburelli, C., Viti, M., 2009. A review on the driving mechanism of the Tyrrhenian-Apennines system: Implications for the present seismotectonic setting in the Central-Northern Apennines. Tectonophysics 476, 22–40. https://doi.org/10.1016/j.tecto.2008.10.032

Martínez-Martínez, J., Corbí, H., Martin-Rojas, I., Baeza-Carratalá, J.F., Giannetti, A., 2017. Stratigraphy, petrophysical characterization and 3D geological modelling of the historical quarry of Nueva Tabarca island (western Mediterranean): Implications on heritage conservation. Eng. Geol. 231, 88–99. https://doi.org/10.1016/j.enggeo.2017.10.014

Massironi, M., Zampieri, D., Caporali, A., 2006. Miocene to present major fault linkages through the Adriatic indenter and the Austroalpine--Penninic collisional wedge (Alps of NE Italy). Geol. Soc. London, Spec. Publ. 262, 245–258. https://doi.org/10.1144/GSL.SP.2006.262.01.15

Moya, C.E., Raiber, M., Cox, M.E., 2014. Journal of Hydrology: Regional Studies Three-dimensional geological modelling of the Galilee and central Eromanga basins , Australia : New insights into aquifer / aquitard geometry and potential influence of faults on. J. Hydrol. Reg. Stud. 2, 119–139. https://doi.org/10.1016/j.ejrh.2014.08.007

Monterrosa, M., Montalvo López, F.E., 2010. Sustainability analysis of the Ahuachapán geothermal field: Management and modeling. Geothermics 39, 370–381. https://doi.org/10.1016/j.geothermics.2010.09.008

O'Sullivan, M., Yeh, A., Mannington, W., 2010. Renewability of geothermal resources. Geothermics 39, 314–320. https://doi.org/10.1016/j.geothermics.2010.09.003

Painter, S.L., Gable, C.W., Kelkar, S., 2012. Pathline tracing on fully unstructured control-volume grids. Comput. Geosci. 16, 1125–1134. https://doi.org/10.1007/s10596-012-9307-1

Painter, S.L., Coon, E.T., Atchley, A.L., Berndt, M., Garimella, R., Moulton, J.D., Svyatskiy, C.J., 2016. Integrated surface/subsurface permafrost thermal hydrology: model formulation and proof-of-concept simulations. *Water Resour Res*. 52(8), 6062- 6077. 10.1002/2015WR018427

Pasquale, V., Gola, G., Chiozzi, P., Verdoya, M., 2011. Thermophysical properties of the Po Basin rocks. Geophys. J. Int. 186, 69–81. https://doi.org/10.1111/j.1365-246X.2011.05040.x

Pasquale, V., Verdoya, M., Chiozzi, P., 2014. Heat flow and geothermal resources in northern Italy. Renew. Sustain. Energy Rev. 36, 277–285. https://doi.org/10.1016/j.rser.2014.04.075

Passadore, G., Monego, M., Altissimo, L., Sottani, A., Putti, M., Rinaldo, A., 2012. Alternative conceptual models and the robustness of groundwater management scenarios in the multi-aquifer system of the Central Veneto Basin, Italy. Hydrogeol. J. 20, 419–433. https://doi.org/10.1007/s10040-011-0818-y

Pellegrini, G.B., 1988. Aspetti morfologici ed evidenze neotettoniche della linea Schio-Vicenza. Suppl. Geogr. Fis. Dinam. Quat., 1, 69-82.

Piccoli, G., Bellati, R., Binotti, C., Lallo, E., Sedea, R., Dal Pra`, A., Cataldi, R., Gatto, G., Ghezzi, G., Marchetti, M., Bulgarelli, G., Schiesaro, G., Panichi, C., Tongiorgi, E., Baldi, P., Ferrara, G.C., Medizza, F., Norinelli, A., De Vecchi, G., Gregnanin, A., Sbettega, G., 1976. Il sistema idrotermale euganeo-berico e la geologia dei Colli Euganei. Mem. Ist. Geol. Miner. Padova, vol 30. Padova, 266pp.

Piccoli, G., Sedea, R., Bellati, R., Di Lallo, E., Medizza, F., Girardi, A., de Pieri, R., De Vecchi, G., Gregnanin, A., Piccirillo, E.M., Norinelli, A., Dal Prà, A., 1981. Note illustrative della carta geologica dei Colli Euganei alla scala 1: 25.000. Mem. di Sci. Geol.

Pilli, A., Sapigni, M., Zuppi, G.M., 2012. Karstic and alluvial aquifers: A conceptual model for the plain - Prealps system (northeastern Italy). J. Hydrol. 464–465, 94–106. https://doi.org/10.1016/j.jhydrol.2012.06.049

Pola, M., Ricciato, A., Fantoni, R., Fabbri, P., Zampieri, D., 2014a. Architecture of the western margin of the North Adriatic foreland: The Schio-Vicenza fault system. Ital. J. Geosci. 133, 223–234. https://doi.org/10.3301/IJG.2014.04

Pola, M., Gandin, A., Tuccimei, P., Soligo, M., Deiana, R., Fabbri, P., Zampieri, D., 2014b. A multidisciplinary approach to understanding carbonate deposition under tectonically controlled hydrothermal circulation: A case study from a recent travertine mound in the Euganean hydrothermal system, northern Italy. Sedimentology 61, 172–199. https://doi.org/10.1111/sed.12069

Pola, M., Fabbri, P., Piccinini, L., Marcolongo, E., Rosignoli, A., Zampieri, D., Roghel, A., Onisto, S., Zampieri, E., 2015a. Anthropic impact on thermal aquifer: the case study of the Euganean Geothermal Field (NE Italy). Rend. online della Soc. Geol. Ital. 35, 240–243. https://doi.org/10.3301/ROL.2015.110

Pola, M., Fabbri, P., Piccinini, L., Zampieri, D., 2015b. Conceptual and numerical models of a tectonically-controlled geothermal system: a case study of the Euganean Geothermal System, Northern Italy. Cent. Eur. Geol. 58, 129–151. http://dx.doi.org/ 10.1556/24.58.2015.1-2.9.

Pola, M., Cacace, M., Fabbri, P., Piccinini, L., Zampieri, D., Torresan, F., 2020. Fault control on a thermal anomaly: conceptual and numerical modelling of a low-temperature geothermal system in the Southern Alps foreland basin (NE Italy). Journal of Geophysical Research: Solid Earth

Rotevatn, A., Peacock, D.C.P., 2018. Strike-slip reactivation of segmented normal faults: Implications for basin structure and fluid flow. Basin Research, (June). https://doi.org/10.1111/bre.12303

Rowland, J. V., Sibson, R.H., 2004. Structural controls on hydrothermal flow in a segmented rift system, Taupo Volcanic Zone, New Zealand. Geofluids 4, 259–283. doi:10.1111/j.1468-8123.2004.00091.x.

Rybach, L., 2003. Geothermal energy: Sustainability and the environment. Geothermics 32, 463–470. https://doi.org/10.1016/S0375-6505(03)00057-9

Rybach, L., Mongillo, M., 2006. Geothermal Sustainability-A Review with Identified Research Needs. GRC Trans. 30, 1083–1090. https://doi.org/10.1177/0146167200268006

Savage, H.M., Brodsky, E.E., 2011. Collateral damage: Evolution with displacement of fracture distribution and secondary fault strands in fault damage zones. Journal of Geophysical Research: Solid Earth 116, doi:10.1029/2010JB007665.

Sedea, R., Di Lallo, E., 1984. Carta Geologica dell’area di Valli del Pasubio – Posina – Laghi 1:20,000. S.E.L.C.A., Firenze.

Stefansson, V., 2000. The renewability of geothermal energy. World Geotherm. Congr. 883–888.

Thierry, P., Prunier-Leparmentier, A.M., Lembezat, C., Vanoudheusden, E., Vernoux, J.F., 2009. 3D geological modelling at urban scale and mapping of ground movement susceptibility from gypsum dissolution: The Paris example (France). Eng. Geol. 105, 51–64. https://doi.org/10.1016/j.enggeo.2008.12.010

Touch, S., Likitlersuang, S., Pipatpongsa, T., 2014. 3D geological modelling and geotechnical characteristics of Phnom Penh subsoils in Cambodia. Eng. Geol. 178, 58–69. https://doi.org/10.1016/j.enggeo.2014.06.010

Veneto Region, 2019. Veneto Region WEB Gis (IDT-RV 2.0 – Infrastruttura dati territoriale della Regione del Veneto). https://idt2.regione.veneto.it/, (accessed October 2017 – December 2019)

VIDEPI Project, 2007. Visibilità dei dati afferenti all'attività di esplorazione petrolifera in Italia (Visibility of petroleum exploration data in Italy). https://www.videpi.com/ (accessed October - November 2017)

Volpi, G., De Caro, M., Crosta, G.B., Magri, F., Fisher, T., Colucci, F., 2018. Modeling Highly Buoyant Flows in the Castel Giorgio: Torre Alfina Deep Geothermal Reservoir. Geofluids 2018, 19pp. https://doi.org/10.1155/2018/3818629

Zampieri, D., Massironi, M., 2007. Evolution of a poly-deformed relay zone between fault segments in the eastern Southern Alps, Italy. Geol. Soc. London, Spec. Publ. 290, 351–366. https://doi.org/10.1144/SP290.13

Zampieri, D., Massironi, M., Sedea, R., Sparacino, V., 2003. Strike-slip contractional stepovers in the Southern Alps (Northeastern Italy). Eclogae Geol. Helv. https://doi.org/10.1007/S00015-003-1070-9

Zampieri, D., Fabbri, P., Pola, M., 2009. Structural constraints to the Euganean Geothermal Field (NE Italy). Rend. Online Soc. Geol. Ital. 5, 238–240.

Zattin, M., Cuman, A., Fantoni, R., Martin, S., Scotti, P., Stefani, C., 2006. From Middle Jurassic heating to Neogene cooling: The thermochronological evolution of the Southern Alps. Tectonophysics 414, 191–202. https://doi.org/10.1016/j.tecto.2005.10.020

Zhang, Q., Zhu, H., 2018. Collaborative 3D geological modeling analysis based on multi-source data standard. Eng. Geol. 246, 233–244. https://doi.org/10.1016/j.enggeo.2018.10.001